

Tropical forests are approaching critical temperature thresholds

<https://doi.org/10.1038/s41586-023-06391-z>

Received: 31 August 2021

Accepted: 30 June 2023

Published online: 23 August 2023

 Check for updates

Christopher E. Doughty^{1✉}, Jenna M. Keany¹, Benjamin C. Wiebe¹, Camilo Rey-Sanchez², Kelsey R. Carter^{3,4}, Kali B. Middleby⁵, Alexander W. Cheesman⁵, Michael L. Goulden⁶, Humberto R. da Rocha⁷, Scott D. Miller⁸, Yadvinder Malhi⁹, Sophie Fauset¹⁰, Emanuel Gloor¹¹, Martijn Slot¹², Imma Oliveras Menor^{9,13}, Kristine Y. Crous¹⁴, Gregory R. Goldsmith¹⁵ & Joshua B. Fisher¹⁵

The critical temperature beyond which photosynthetic machinery in tropical trees begins to fail averages approximately 46.7 °C (T_{crit})¹. However, it remains unclear whether leaf temperatures experienced by tropical vegetation approach this threshold or soon will under climate change. Here we found that pantropical canopy temperatures independently triangulated from individual leaf thermocouples, pyrgeometers and remote sensing (ECOSTRESS) have midday peak temperatures of approximately 34 °C during dry periods, with a long high-temperature tail that can exceed 40 °C. Leaf thermocouple data from multiple sites across the tropics suggest that even within pixels of moderate temperatures, upper canopy leaves exceed T_{crit} 0.01% of the time. Furthermore, upper canopy leaf warming experiments (+2, 3 and 4 °C in Brazil, Puerto Rico and Australia, respectively) increased leaf temperatures non-linearly, with peak leaf temperatures exceeding T_{crit} 1.3% of the time (11% for more than 43.5 °C, and 0.3% for more than 49.9 °C). Using an empirical model incorporating these dynamics (validated with warming experiment data), we found that tropical forests can withstand up to a 3.9 ± 0.5 °C increase in air temperatures before a potential tipping point in metabolic function, but remaining uncertainty in the plasticity and range of T_{crit} in tropical trees and the effect of leaf death on tree death could drastically change this prediction. The 4.0 °C estimate is within the ‘worst-case scenario’ (representative concentration pathway (RCP) 8.5) of climate change predictions² for tropical forests and therefore it is still within our power to decide (for example, by not taking the RCP 6.0 or 8.5 route) the fate of these critical realms of carbon, water and biodiversity^{3,4}.

Tropical forest mean temperatures are high, and their diel and seasonal variations are relative small, thus even a small change in temperature could more greatly impact tropical plant species than a large temperature change in other global regions⁵. Average temperatures have risen by 0.5 °C per decade in some tropical regions, and temperature extremes are becoming more pronounced (for example, the El Niño of 2015 was 1.5 °C warmer than the El Niño of 1997)^{6,7}. As temperatures in tropical forests are near or above the temperature optimum for photosynthesis⁸, further increased temperatures may close stomata, reducing transpirational cooling and exposing leaves to damaging temperatures. More than 150 years ago, Sachs (1864) first reported that leaves from different plant species could withstand temperatures

of up to 50 °C, but would die at temperatures even slightly higher⁹. In the era of climate change, this finding is still relevant. How close forests are to a high temperature threshold such as the one proposed by Sachs is a particularly important issue in tropical forests, which serve as critical stores and sinks of carbon, are host to most of the world’s biodiversity and may be more sensitive to increasing temperatures than other ecoregions^{3,4}.

More recently, techniques to determine the ability for leaves to withstand high temperatures have advanced to focus on T_{crit} , or the temperature at which irreversible damage to the photosynthetic machinery occurs. Over the past few years, T_{crit} data have become increasingly available for tropical forests, specifically measured as the temperature

¹School of Informatics, Computing, and Cyber Systems, Northern Arizona University, Flagstaff, AZ, USA. ²Department of Marine, Earth and Atmospheric Sciences, North Carolina State University, Raleigh, NC, USA. ³College of Forest Resources and Environmental Sciences, Michigan Technological University, Houghton, MI, USA. ⁴Earth and Environmental Sciences Division, Los Alamos National Laboratory, Los Alamos, NM, USA. ⁵Centre for Tropical Environmental and Sustainability Science, James Cook University, Cairns, Queensland, Australia. ⁶Department of Earth System Science, University of California, Irvine, CA, USA. ⁷Departamento de Ciências Atmosféricas, Universidade de São Paulo, São Paulo, Brazil. ⁸Atmospheric Sciences Research Center, State University of New York at Albany, Albany, NY, USA. ⁹Environmental Change Institute, School of Geography and the Environment, University of Oxford, Oxford, UK. ¹⁰School of Geography, Earth and Environmental Sciences, University of Plymouth, Plymouth, UK. ¹¹University of Leeds, Leeds, UK. ¹²Smithsonian Tropical Research Institute, Balboa, Ancon, Republic of Panama. ¹³AMAP (Botanique et Modélisation de l’Architecture des Plantes et des Végétations), CIRAD, CNRS, INRA, IRD, Université de Montpellier, Montpellier, France. ¹⁴Western Sydney University, Hawkesbury Institute for the Environment, Penrith, New South Wales, Australia. ¹⁵Schmid College of Science and Technology, Chapman University, Orange, CA, USA. ✉e-mail: chris.doughty@nau.edu

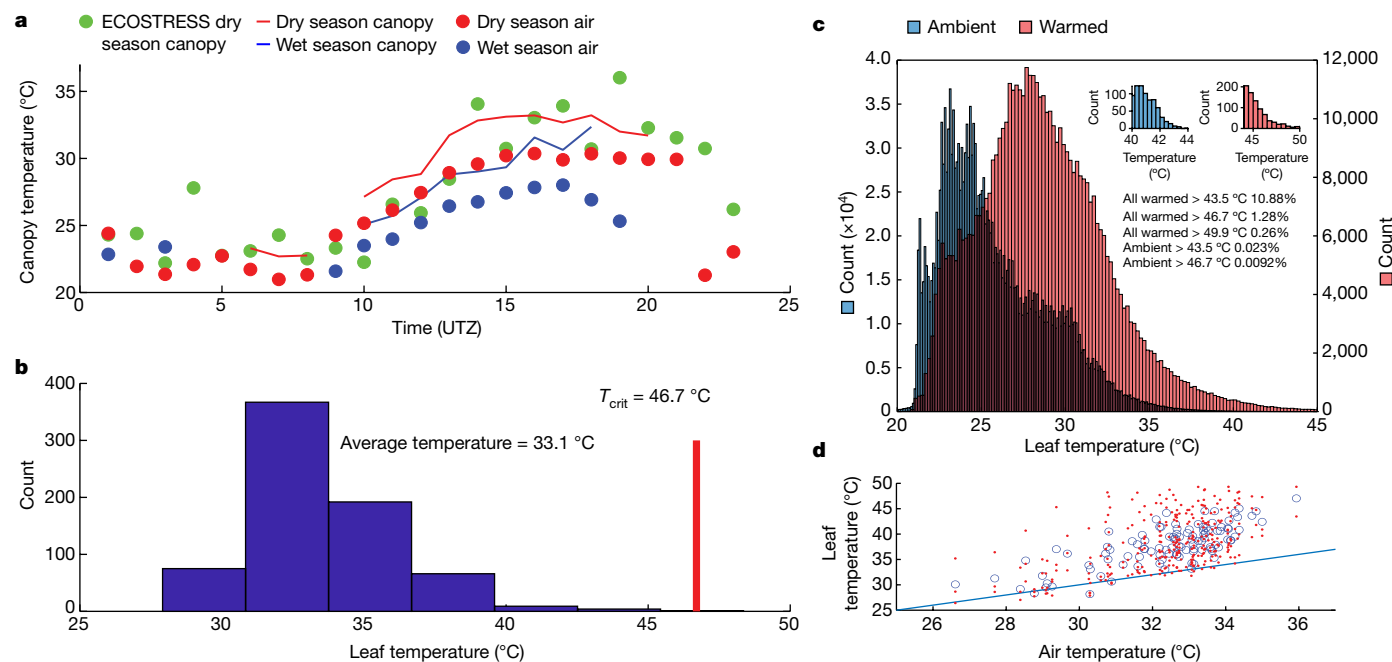


Fig. 1 | In situ and warming experiment leaf temperatures compared with canopy temperatures. **a**, Diurnal temperature patterns for the dry season for a region (Supplementary Fig. 1a) of the Amazon basin using ECOSTRESS data (green). Average canopy (solid line) and 40-m air temperatures (circles) from the KM 83 eddy covariance tower for the dry season (red) and the wet season (blue) for sunny periods (when $solar_{in}/solar_{in,max}$ is more than 90% for the hour). **b**, Histogram of individual canopy top leaf thermocouples from 11 individual leaves from the same site as in **a** over 54 sunny periods lasting 20 min

(measurements were taken every 2 min) and the average of these data (33.1 °C). T_{crit} is the temperature when the photosynthetic machinery breaks down and is shown as a red line. **c**, We aggregated all leaf thermocouple data from Supplementary Fig. 7 for ambient (blue) and warmed leaves (red) and show the percentage of leaves at +2 °C (Brazil), +3 °C (Puerto Rico) and +4 °C (Australia) warming that were more than T_{crit} . **d**, Air temperature versus leaf temperature for a warming experiment for individual leaves (red dots), average leaf temperatures (blue circles) and one-to-one line (blue).

at which the ratio of variable fluorescence yield to maximum fluorescence yield (F_v/F_m), reflecting photosystem II functioning, starts to decline^{1,10}. The decline in F_v/F_m is often followed by the development of necrosis and leaf death¹¹. Heat tolerance, measured by T_{crit} , varies minimally among tropical species, mainly due to differences in growing environment and leaf traits. For instance, among 147 tropical tree species, the average T_{crit} was found to be 46.7 °C (5–95th percentile: 43.5–49.7 °C)¹. They also found that older tree lineages that experienced higher temperatures in the distant past did not have higher T_{crit} and thus were not better acclimated to the higher temperatures of today. Across the planet, heat tolerance generally increases with higher mean growing temperatures. For example, as average temperatures increase by approximately 20 °C from the Arctic to the Tropics, heat tolerance was 9 °C greater in tropical plants than in Arctic plants¹². Similarly, as temperatures decrease by 17 °C along a tropical elevation gradient, heat tolerance decreases by approximately 2 °C¹⁰. Heat tolerance also increases with increasing leaf mass area, suggesting that heat tolerance may be linked to construction costs of the leaves and their mean leaf lifetime¹.

With a much-improved understanding of T_{crit} across the Tropics, it is now important to know how close tropical leaves are to experiencing and surpassing these critical temperatures. In the past, tropical forest leaf and canopy temperatures were difficult and time consuming to measure, but new technologies such as drones and thermal cameras are making the process much easier¹³. More recently, the Ecosystem Spaceborne Thermal Radiometer Experiment on Space Station (ECOSTRESS) sensor on the International Space Station can provide unique high temporal and spatial resolution measurements of land surface temperatures (LSTs) at the global scale¹⁴. ECOSTRESS is an improvement over previous thermal satellite LST sensors because it has five spectral bands, a 70-m spatial resolution and multiple diel overpass times, as well as improved algorithms.

Here we used data from the new ECOSTRESS sensor to estimate peak pantropical forest canopy temperatures. We began by ground truthing the satellite data with tower-based pyrgeometer data. We then used these data to determine what causes variation in peak temperatures at the canopy scale and show similar trends driving peak temperatures across all of the Tropics. Critically, we show that for a given canopy temperature, individual leaf temperatures display a ‘long tail’ of values in the distribution, in which the temperatures of a few individual leaves far exceed that of the overall canopy, and that this skewed distribution persists under leaf warming experiments of 2, 3 and 4 °C. Finally, we developed a simple empirical model to explore the implications of observed leaf temperatures on the fate of tropical forests under future climate change.

Ground validation

Using pyrgeometer data, we first ground truth ECOSTRESS and found similar peak temperatures between a 3-year, 30-min averaged canopy temperature pyrgeometer dataset for a lowland tropical rainforest site near the Tapajos River (KM 83 eddy covariance tower) in Brazil and a broad region (Extended Data Fig. 1a, red box) of the Amazon basin (Fig. 1a; $r^2 = 0.75$, $n = 16$, $P < 0.0001$, with ECOSTRESS having a slight cool bias (Extended Data Fig. 2d) matching previous findings¹³). The pyrgeometer data at that site indicate that midday sunny canopy temperatures in the dry season (July to December) averaged 33.5 °C compared with 31.0 °C in the wet season (January to June) (Fig. 1a). Sampling frequency (Extended Data Fig. 3), latent heat flux (Extended Data Fig. 2c), air temperature (Extended Data Fig. 2b) and soil moisture (Extended Data Fig. 2a) all impacted canopy temperatures. The tower-mounted pyrgeometer inherently averages spatially (over a footprint of 8,000 m²) and thus amalgamates individual peak leaf temperatures. Therefore, we used leaf thermocouples on three canopy tree

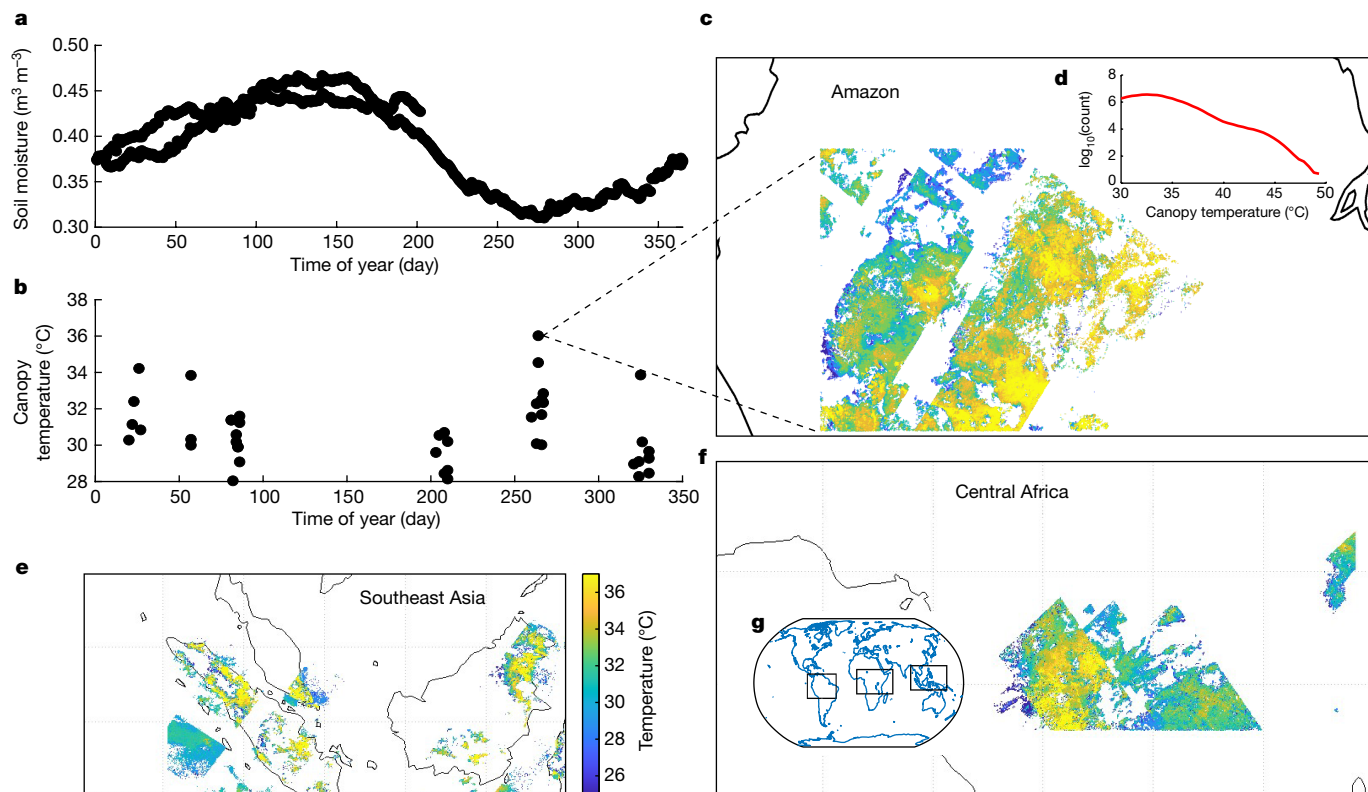


Fig. 2 | Remotely sensed peak canopy temperature across the tropics. **a, b**, Seasonal patterns of soil moisture using SMAP (**a**) and canopy temperatures using ECOSTRESS (**b**) for the Amazon basin (Extended Data Fig. 1a, red). **c, d**, For the hot dry period shown by the black dashed lines, we show a larger spatial distribution (**c**) (Extended Data Fig. 1a, green) and \log_{10}

histogram focusing on the long tail of the data (**d**) using only the highest quality data flag. **e, f**, Trends for periods of low soil moisture for the Southeast Asian region (**e**) (Extended Data Fig. 8) and Central Africa (**f**) (Extended Data Fig. 7). **g**, A world map with focal areas boxed in black.

species at the same site to assess individual leaf temperatures. The mean temperatures for 11 individual sun-exposed leaves over 54 sunny 20-min periods also averaged approximately 33.1 °C (similar to that measured by the pyrgeometer) but with a 'long tail' of high temperatures (more than 40 °C) in the distribution (Fig. 1b).

We then aggregated similar upper canopy leaf thermocouple datasets from Brazil^{16,17}, Puerto Rico¹⁸, Panama¹⁹ and Australia²⁰ and all had long-tail distributions (Fig. 1c and Extended Data Figs. 4 and 5) with upper limits of approximately 44 °C (ranging between 43 and 48 °C) (but see Extended Data Fig. 5c for an example of a cooler Atlantic forest¹⁶). When we zoomed in on the long tail of each dataset (insets in Extended Data Figs. 4 and 5), the curve shows statistical regularity, which allowed us to estimate T_{crit} as a percent of all canopy top leaves. For instance, when all data are aggregated across sites, we estimated that 0.01% (0.03% for more than 43.5 °C) of all leaves will surpass T_{crit} at least once a season (Fig. 1c). Although infrequent, the occurrence of extreme temperatures may have a catastrophic effect on the physiology of a leaf and may be thought of as a low-probability, high-impact event.

We then aggregated data from three in situ upper canopy warming experiments in which leaves were heated by 2, 3 and 4 °C (in Brazil¹⁷, Puerto Rico¹⁸ and Australia²⁰, respectively). Warmed leaf peak temperatures ranged between 51 and 54 °C (Extended Data Fig. 4), an increase of approximately 8 °C above ambient highs (mean of approximately 45 °C; Extended Data Fig. 4). The percentage of warmed leaves exceeding T_{crit} at least once a year increased to 1.3% of all warmed leaves (11% for more than 43.5 °C, and 0.3% for more than 49.9 °C) (Fig. 1c) because of a non-linear relationship between leaf and air temperatures in the warming experiments (Fig. 1d). During the Brazilian warming experiment, individual leaves exceeded T_{crit} and T_{50} (the temperature at which F_w/F_m

decreases by 50%) with noticeable signs of leaf necrosis, some for a duration of more than 8 min (Extended Data Fig. 6), and following this, net transpiration in warmed branches decreased significantly ($P < 0.0001$) by an average of 27% (Fig. 3a). In the warming experiments, leaves exceeded T_{crit} for extended periods (more than 8 min) 0.2% (0.6% for more than 6 min) of the time over the course of a season (Extended Data Fig. 6), events that can cause leaf browning and necrosis.

Remote sensing data

We analysed ECOSTRESS LST data along with comparisons to Visible Infrared Imaging Radiometer Suite (VIIRS) and Moderate Resolution Imaging Spectroradiometer (MODIS), as well as soil moisture active passive (SMAP) soil moisture. At the landscape scale (Extended Data Fig. 1, red box), peak ECOSTRESS LST (approximately 36 °C) using all data corresponded with periods of low SMAP-measured soil moisture (approximately 0.3 m³ m⁻³) (Fig. 2a,b). A linear extrapolation of our pyrgeometer data to a soil moisture of 0.3 m³ m⁻³ would predict a similar canopy temperature (approximately 36 °C) (Extended Data Fig. 2a). For the warmest data point (Fig. 2c,d), we then expanded the area (Extended Data Fig. 1, blue box) and applied the highest quality data flags (approximately 6% of the data used; see Methods and Supplementary information for an extensive discussion of this), which reduced the median value to 34 °C. These average temperatures do not reflect the extremes, as 0.5% of the data is more than 38 °C and 0.1% is more than 40 °C (Table 1 and Fig. 2d). We show the long tail distribution of temperatures (with a \log_{10} scale) for Amazonia in Fig. 2d. Using less-restrictive or no quality flags generally resulted in higher tails more than 40 °C (Supplementary Table 2). We compared ECOSTRESS

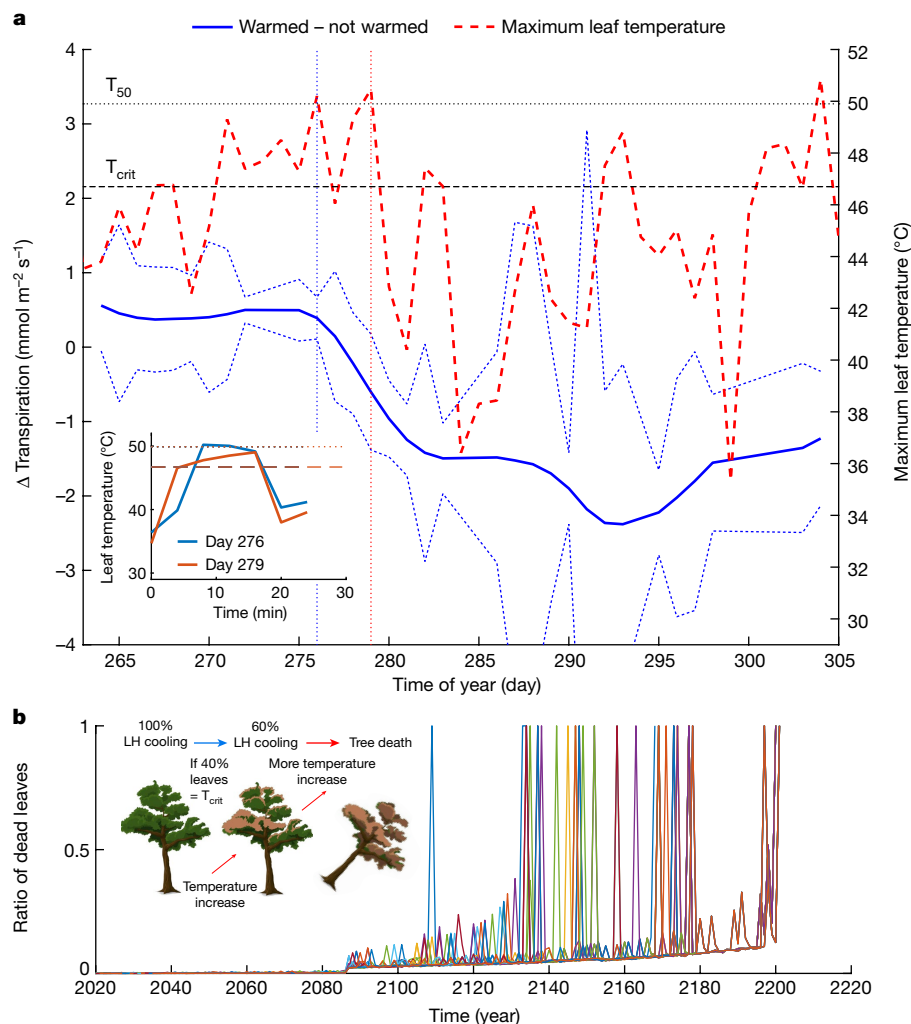


Fig. 3 | Modelled effect of future warming on tropical forests. a, Warmed branch sap flow ($n = 9$ branches) minus non-warmed ($n = 4$ branches) sap flow (blue line) \pm propagated error (blue dotted line) for sunny (irradiance of more than $1,200 \text{ mmol m}^{-2} \text{ s}^{-1}$) midday periods (10:30–14:00 local time) on six tree species using passive black plastic heaters in a heating experiment conducted at Floresta Nacional do Tapajós, Brazil. Maximum daily temperatures for individual leaves (red dashed line) from a co-occurring leaf warming experiment during the same time period. The horizontal black lines indicate T_{crit} (dashed) and T_{50} (dotted). The inset figure shows the duration of warm

periods for days 276 and 279 (marked as vertical red and blue dashed lines). Around this period (between days 276 and 279), transpiration decreases in warmed branches relative to the non-warmed branches. **b**, Dead leaves as a ratio of total leaves over time with climate change for 30 simulations (one colour per simulation) are also shown. The diagram in the inset is of our model showing the effect of T_{crit} on change in average canopy temperature as temperatures increase over time. LH, latent heat. The tree image is from Canva (www.canva.com) under a free content license.

to other LST satellites (VIIRS and MODIS) (Extended Data Figs. 9 and 10 and Supplementary Tables 1 and 2) and showed similar results, but with greater fidelity and ability to capture long tails with ECOSTRESS. LST for Central Africa (Fig. 2f and Extended Data Fig. 7) and Southeast Asia (Fig. 2e and Extended Data Fig. 8) during similar peak dry periods had similar peak temperatures (with data flags; Table 1). We then estimated the highest temperatures during dry periods if temperature increased by 2°C (to simulate climate change) and found that the percent of time above threshold temperatures would increase by an order of magnitude in all three regions. For example, the percent time that Amazon canopies spent at temperatures 38.0°C or more would increase from 0.5 to 5% and the percent time of 40.0°C or more would increase from 0.1 to 1% (Table 1).

Model results

An empirical model to explore the temperature thresholds of tropical trees was parameterized using the temperature distributions of

warmed and non-warmed leaves (Fig. 1c) from the combined tropical datasets ($n = 5$). Assuming leaf death at T_{crit} and evaporative cooling as a linear function of the number of leaves, we show that enhanced warming could tip the forest towards the death of all leaves and possible tree mortality (Table 2 and Fig. 3b). The modelled effect of warming on reduced transpirational cooling approximately matched the measured values; a $26\% (\pm 28\%)$ ($n = 30$ simulations) reduction of modelled evaporative cooling with approximately 2°C warming, versus a measured 27% average reduction after approximately 2°C warming during the Brazilian warming experiment (Fig. 3a). The decline in transpiration occurred after leaf temperatures exceeded both T_{crit} for more than 8 min (Fig. 3a, inset) and T_{50} . Mean initial modelled canopy temperature was $33.7 \pm 0.4^{\circ}\text{C}$, matching the measured canopy average (33.5°C) during peak temperature periods (sunny and midday). When run using the most likely parameters, including a T_{crit} of 46.7°C , the model showed that most forests could withstand up to $3.9 \pm 0.5^{\circ}\text{C}$ warming before the death of all leaves and potential tree death ($n = 30$ simulation runs; Table 2 and Fig. 3b), but a series of sensitivity studies

Table 1 | Current and future temperature extremes across the tropics

Region	38.0 °C or more (%)		40.0 °C or more (%)		45.0 °C or more (%)	
	Current	+2 °C	Current	+2 °C	Current	+2 °C
South America	0.50	5	0.10	1	0	0.10
Central Africa	0.60	2	0.06	0.60	0	0.01
Southeast Asia (Borneo)	3	8	1	3	0.01	0.30

The percentage of time that canopy temperatures are estimated to exceed thresholds of 38.0, 40.0 and 45.0 °C or more for low soil moisture regions of the Amazon, Central Africa and Borneo. We then increased temperature by 2 °C to estimate the effect of climate change and show the same estimates for the three regions. Canopy temperatures are observed by ECOSTRESS and are limited to only the highest quality data.

give a temperature distribution between 2 and 8 °C (Table 2). Owing to the stochastic nature of droughts in our model, total leaf loss ranged over a wide timespan. For instance, if temperatures increase by 0.03 °C per year, we estimate that the mean time to leaf death would be 132 years, but extensive canopy leaf mortality could occur as early as 102 years and as late as 163 years (Table 2 and Fig. 3b).

Discussion

Several lines of remotely sensed, tower-based and in situ evidence (ECOSTRESS, VIIRS, pyrgeometer and leaf thermocouples) suggest that hot periods in tropical forests with low soil moisture lead to canopy temperatures that average approximately 34 °C, with some pixels exceeding 40 °C^{8,21}. Even within a given LST pixel, there is a long-tail distribution with individual leaf temperatures exceeding 40 °C. Currently, 0.01% of upper canopy leaves from in situ measurements exceeded T_{crit} at least once a season ($n = 5$ sites); warming experiments ($n = 3$) suggest 1.4% of upper canopy leaves will exceed T_{crit} under future warming conditions (Fig. 1c). We posit that capturing the higher tail temperatures may be important for future climate change predictions in tropical forests, because as individual leaves exceed T_{crit} , they die, thus reducing the net evaporative cooling potential for the canopy (as suggested in Figs. 1d and 3a). This is supported by branch warming experiments in which noticeable signs of leaf damage and a reduction of transpiration by 27% followed periods in which leaf temperatures exceeded T_{crit} for extended periods (Fig. 3a). Certain tropical regions, such as the Southeast Amazon, may already be experiencing critical thresholds²². Many recent large-scale drought studies have shown that the largest, most sun-exposed trees die disproportionately^{23,24}. Moreover, there has been a recent increase in continental mortality across the Amazon basin (although not in the Congo basin; Table 1 shows that the Congo

basin experiences lower peak temperatures than the Amazon)⁴ and carbon uptake across the basin has been reduced²⁵. We propose that high leaf temperatures may have a role (along with carbon starvation and hydraulic limitation²⁶) in those recent mortality events.

We make several assumptions in our model related to the broader tipping point results. The first key assumption is that within a given LST pixel, there is a long tail of high individual tropical leaf temperatures following Fig. 1c. This is supported by several leaf thermocouple datasets ($n = 5$; Fig. 1 and Extended Data Figs. 4 and 5), all of which show a long tail, as well as first principles (Supplementary text). Critically, warming experiments show non-linear trends (Fig. 1c,d) in which temperature increases of 2, 3 and 4 °C increase maximum leaf temperatures by larger amounts (+8.1, +6.1 and 8.0 °C, respectively; Extended Data Fig. 4). Many other studies have documented individual leaf temperatures approaching 46.7 °C^{8,11,17,19}.

The second assumption is that water-stressed pantropical median canopy temperatures can average approximately 34 °C with a spatial tail exceeding 40 °C (Fig. 2). In other words, remote sensing data suggest that entire canopies and forests are getting very warm and (our first assumption) that within these pixels there is a long-tail distribution of individual leaf temperatures. ECOSTRESS and VIIRS LST data are both more than 1 °C warmer (34.7 and 33.9 °C) than older LST sensors such as MODIS (32.7 °C) (ECOSTRESS has approximately 0.75 °C cold bias compared with VIIRS¹⁵). We assume ECOSTRESS and VIIRS will be more accurate than MODIS because there are more thermal bands, vegetation can be identified with emissivity (for ECOSTRESS and VIIRS, but not for MODIS) and an improved algorithm²⁷ can accurately estimate temperatures within 1 K for many surfaces²⁸. We further found that adding 2 °C (to replicate climate change) to the measured ECOSTRESS satellite data would increase the occurrence of high-tail temperatures by about an order of magnitude (for example, from 0.1 to 1% for more than 40 °C) (Table 1). Therefore, the change in percentage of time when temperatures exceeded more than 40 °C in response to a simple addition of 2 °C was not a simple linear change.

The third assumption is that leaves at temperatures more than T_{crit} will die, and thus stop contributing to future transpiration (although transpiration often stops at temperatures lower than T_{crit}), and that the sum of evaporative cooling is a linear function of the total number of transpiring leaves. Our T_{crit} value is based on Slot et al.¹, who found the mean (T_{crit}) was 46.7 °C (5–95th percentile: 43.5–49.7 °C) and the temperature when F_s/F_m had decreased by 50% (T_{50}) was 49.9 °C (47.8–52.5 °C)¹. T_{crit} variation is important because approximately 50% of the species from Slot et al.¹ had a T_{crit} of less than 46.7 °C with negative consequences at lower temperatures for those species. Incorporating this variation in our model demonstrated that those consequences could exacerbate conditions for other species as they die and their evaporative cooling is reduced, leading to less future warming (approximately 0.1 °C) needed to achieve leaf death when such variation is included (Table 2). Branch

Table 2 | Results from model sensitivity studies

Most likely scenario ($T_{crit}=46.7$)	Drought		T_{crit}	T_{crit} range	T_{crit} duration	Soil moisture coefficient	Maximum evaporation cooling		
LAI 5	5%	20%	45 °C	49.9 °C	46.7 ± 2 °C	More than three periods	3.7 °C		
Total temperature increase (°C)	3.9 ± 0.5	3.6 ± 0.7	4.9 ± 1.1	2.6 ± 0.6	7.3 ± 0.8	3.8 ± 0.7	4.7 ± 0.8	4.1 ± 0.7	5.2 ± 0.5
Timescale until leaf death (years)	132 (102–163)	120 (88–170)	163 (108–238)	89 (69–133)	244 (204–300)	131 (100–185)	159 (129–220)	138 (91–183)	173 (145–202)

An individual-based model showing the estimated amount of climate change under different scenarios before leaf death. The results from the 'most likely scenario' with an LAI of 5, 10% drought probability, 46.7 °C T_{crit} , T_{crit} range=0, T_{crit} duration=1, a soil moisture exponent of -33.6, and maximum evaporative cooling of 4.4 °C are first shown. Then, the results of contrasting extreme scenarios as a means of a sensitivity analysis in which we keep all other variables as in the 'most likely scenario', but vary the one mentioned are shown. Temperature increase results represent means ± 1 s.d., whereas timescale results represent means and range in parentheses ($n=30$ simulation runs).

warming experiments in Brazil showed large (27%) decreases in transpiration when leaves reached either T_{50} or T_{crit} for an extended period (more than 8 min) (Fig. 3). It was not possible to determine which (T_{50} , extended T_{crit} or a different variable) was more critical for the decrease in transpiration in our dataset (but another recent study has found leaf death when leaf temperatures exceeded T_{crit} for between 10 and 40 min (ref. 29)). If a longer time is necessary to exceed T_{crit} before leaf death, T_{crit} will be exceeded less often and our model suggests that the forest canopies could resist an additional 0.8 °C increase in air temperatures before leaf death (Table 2). Previous work had suggested that irreversible damage will often occur at 45–60 °C³⁰.

T_{crit} was the largest source of uncertainty in the model and changed the tipping point temperatures by between 2 and 8 °C (Table 2). T_{crit} has been adopted because it is relatively easy to measure and can be standardized across ecosystems. However, the effect of T_{crit} on plant hydraulics still needs more research³¹. Other uncertainties include the importance of T_{crit} versus T_{50} on enzyme denaturation and how long exposure to high temperatures is needed for enzyme denaturation to occur¹. We also assumed that T_{crit} does not acclimate to warming—acclimation has been observed in temperate species³², but the few studies that have examined acclimation in tropical species found no or very limited evidence for upregulation of T_{crit} ^{11,33} (although warm-selected tropical trees in Biosphere 2 did show acclimation of T_{crit} ³⁴). In a sensitivity study, we allowed acclimation by enabling leaves to increase T_{crit} by 0.5 or 1 °C, which increased forest resistance to warming by similar amounts (by 0.5 and 1 °C).

An additional assumption was that if all leaves die at T_{crit} , the tree will die. However, tropical trees may use non-structural carbohydrate^{26,35} reserves to reflush leaves in later years, but this is highly uncertain. Given these uncertainties, we made the simple assumption that leaf-level T_{crit} is a general signal of enzyme denaturation (supported by ref. 36), which will have a range of other impacts, including reducing evaporative cooling and possibly leading to tree death. It is clear that further studies are needed. However, in a sensitivity study, we tried to account for high non-structural carbohydrates by allowing trees to reflush a leaf area index (LAI) of 2 (for example, increase total LAI to 7), which slightly increased resilience by 0.2 °C (Supplementary text). We also assume that all sunlit leaves have an equal chance of dying, but leaf orientation probably impacts both leaf temperatures and T_{crit} and only further studies may address this. If the assumptions above are robust, then our model suggests that tropical forests may be approaching a high temperature threshold.

How close future predictions of temperature increases in tropical forests are to our predictions of leaf death is to be determined. An ensemble of Coupled Model Intercomparison Project (CMIP5) models (with similar results from CMIP6 (ref. 37)), the ‘worst-case scenario’ (RCP 8.5) predicts temperature increases of 3.3 ± 0.6 °C by 2081–2100 for tropical regions, with land regions heating by approximately 5 °C by 2181 in RCP 6.0 and by 2081 in RCP 8.5 (ref. 2). This level of climate change is within the range of our most likely scenario of 3.9 ± 0.50 °C of temperature increases that lead to a tipping point. However, the 4 °C is out of the range of the ‘best-case scenario’ (RCP 2.6) of 0.9 ± 0.3 °C, or 1.4 ± 0.5 °C for the land surface. Tree death could come earlier through a combination of mechanisms and their interactions (for example, carbon starvation, hydraulic limitation and fire, among others). Furthermore, even at lower temperatures, partial canopy death can negatively affect CO₂ uptake feedbacks, which could accelerate climate change effects. Our sensitivity study (Table 2) shows temperature ranges leading to leaf death between approximately 2.0 and 8.1 °C (the lowest and highest scenarios plus error). Scenario uncertainty due to the change in drought prevalence had a relatively small role, shifting our best estimate by approximately 0.4 °C. Most of this uncertainty is methodological (T_{crit} value and high temperature duration), which could be reduced with further studies and method standardization of T_{crit} measurements.

Conclusion

Our work suggests that a tipping point in metabolic function in tropical forests could occur with 3.9 ± 0.5 °C of additional warming, which is more than expected for tropical forests under RCP 2.6, but less than under RCP 6.0 or 8.5. We used T_{crit} to simplify an enormously complex process and we want to emphasize that even our great uncertainty (2–8 °C) estimates may ignore critical feedbacks such as sensitivity of reproduction to high temperatures, hydraulic failure due to embolisms and, more generally, other unexplored positive-feedback loops. Recent literature has suggested a resilience of tropical forests to how warming impacts carbon uptake³⁴ (but see ref. 25) and long-term drought³⁸. However, T_{crit} acts as an absolute upper limit and it seems that, if our assumptions in the model are correct, crossing such a threshold is within the range of our most pessimistic future climate change scenarios (RCP 6.0 or 8.5). In addition, deforestation and fragmentation can amplify local temperature changes³⁹. The combination of climate change and local deforestation may already be placing the hottest tropical forest regions close to, or even beyond, a critical thermal threshold⁴⁰. Therefore, our results suggest that the combination of ambitious climate change mitigation goals and reduced deforestation can ensure that these important realms of carbon, water and biodiversity^{3,4} stay below thermally critical thresholds.

Online content

Any methods, additional references, Nature Portfolio reporting summaries, source data, extended data, supplementary information, acknowledgements, peer review information; details of author contributions and competing interests; and statements of data and code availability are available at <https://doi.org/10.1038/s41586-023-06391-z>.

- Slot, M. et al. Leaf heat tolerance of 147 tropical forest species varies with elevation and leaf functional traits, but not with phylogeny. *Plant. Cell Environ.* **44**, 2414–2427 (2021).
- IPCC. *Climate Change 2013: The Physical Science Basis* (eds Stocker, T. F. et al.) (Cambridge Univ. Press, 2013).
- Wilson, E. & Raven, P. in *Biodiversity* (ed. Wilson, E. O.) Ch. 3 (National Academy Press, 1988).
- Hubau, W. et al. Asynchronous carbon sink saturation in African and Amazonian tropical forests. *Nature* **579**, 80–87 (2020).
- Janzen, D. H. Why mountain passes are higher in the Tropics. *Am. Nat.* **101**, 233–249 (1967).
- Jiménez-Muñoz, J. C. et al. Record-breaking warming and extreme drought in the Amazon rainforest during the course of El Niño 2015–2016. *Sci. Rep.* **6**, 33130 (2016).
- Jiménez-Muñoz, J. C., Sobrino, J. A., Mattar, C. & Malhi, Y. Spatial and temporal patterns of the recent warming of the Amazon forest. *J. Geophys. Res. Atmos.* **118**, 5204–5215 (2013).
- Doughty, C. E. & Goulden, M. L. Are tropical forests near a high temperature threshold? *J. Geophys. Res.* <https://doi.org/10.1029/2007JG000632> (2008).
- Sachs, J. Über die obere temperaturgränze der vegetation. *Flora* **47**, 5–12 (1864).
- Feeley, K. et al. The thermal tolerances, distributions, and performances of tropical montane tree species. *Front. For. Glob. Change* **3**, 25 (2020).
- Krause, G. H. et al. High-temperature tolerance of a tropical tree, *Ficus insipida*: methodological reassessment and climate change considerations. *Funct. Plant Biol.* **37**, 890–900 (2010).
- O’Sullivan, O. S. et al. Thermal limits of leaf metabolism across biomes. *Glob. Chang. Biol.* **23**, 209–223 (2017).
- Still, C. J. et al. Imaging canopy temperature: shedding (thermal) light on ecosystem processes. *New Phytol.* **230**, 1746–1753 (2021).
- Fisher, J. B. et al. ECOSTRESS: NASA’s next generation mission to measure evapotranspiration from the International Space Station. *Water Resour. Res.* **56**, e2019WR026058 (2020).
- Hulley, G. C. et al. Validation and quality assessment of the ECOSTRESS level-2 land surface temperature and emissivity product. *IEEE Trans. Geosci. Remote Sens.* **60**, 1–23 (2022).
- Fauset, S. et al. Differences in leaf thermoregulation and water use strategies between three co-occurring Atlantic forest tree species. *Plant. Cell Environ.* **41**, 1618–1631 (2018).
- Doughty, C. E. An in situ leaf and branch warming experiment in the Amazon. *Biotropica* **43**, 658–665 (2011).
- Carter, K. R., Wood, T. E., Reed, S. C., Butts, K. M. & Cavaleri, M. A. Experimental warming across a tropical forest canopy height gradient reveals minimal photosynthetic and respiratory acclimation. *Plant. Cell Environ.* **44**, 2879–2897 (2021).
- Rey-Sanchez, A. C., Slot, M., Posada, J. & Kitajima, K. Spatial and seasonal variation of leaf temperature within the canopy of a tropical forest. *Clim. Res.* **71**, 75–89 (2016).
- Crous, K. Y. et al. Similar patterns of leaf temperatures and thermal acclimation to warming in temperate and tropical tree canopies. *Tree Physiol.* tpad054 (2023).

21. Kivalov, S. N. & Fitzjarrald, D. R. Observing the whole-canopy short-term dynamic response to natural step changes in incident light: characteristics of tropical and temperate forests. *Boundary Layer Meteorol.* **173**, 1–52 (2019).
22. Tiwari, R. et al. Photosynthetic quantum efficiency in south-eastern Amazonian trees may be already affected by climate change. *Plant. Cell Environ.* **44**, 2428–2439 (2021).
23. da Costa, A. C. L. et al. Effect of 7 yr of experimental drought on vegetation dynamics and biomass storage of an eastern Amazonian rainforest. *New Phytol.* **187**, 579–591 (2010).
24. Phillips, O. L. et al. Drought sensitivity of the Amazon rainforest. *Science* **323**, 1344–1347 (2009).
25. Gatti, L. V. et al. Amazonia as a carbon source linked to deforestation and climate change. *Nature* **595**, 388–393 (2021).
26. Doughty, C. E. et al. Drought impact on forest carbon dynamics and fluxes in Amazonia. *Nature* **519**, 78–82 (2015).
27. Hulley, G. C. & Hook, S. J. Generating consistent land surface temperature and emissivity products between ASTER and MODIS data for Earth science research. *IEEE Trans. Geosci. Remote Sens.* **49**, 1304–1315 (2011).
28. Gillespie, A. et al. A temperature and emissivity separation algorithm for advanced spaceborne thermal emission and reflection radiometer (ASTER) images. *IEEE Trans. Geosci. Remote Sens.* **36**, 1113–1126 (1998).
29. Kitudom, N. et al. Thermal safety margins of plant leaves across biomes under a heatwave. *Sci. Total Environ.* **806**, 150416 (2022).
30. Berry, J. & Bjorkman, O. Photosynthetic response and adaptation to temperature in higher plants. *Annu. Rev. Plant Physiol.* **31**, 491–543 (1980).
31. Blonder, B. & Michaletz, S. T. A model for leaf temperature decoupling from air temperature. *Agric. For. Meteorol.* **262**, 354–360 (2018).
32. Drake, J. E. et al. Trees tolerate an extreme heatwave via sustained transpirational cooling and increased leaf thermal tolerance. *Glob. Chang. Biol.* **24**, 2390–2402 (2018).
33. Guha, A. et al. Short-term warming does not affect intrinsic thermotolerance but induces strong sustaining photoprotection in tropical evergreen citrus genotypes. *Plant. Cell Environ.* **45**, 105–120 (2022).
34. Smith, M. N. et al. Empirical evidence for resilience of tropical forest photosynthesis in a warmer world. *Nat. Plants* **6**, 1225–1230 (2020).
35. Dickman, L. T. et al. Homeostatic maintenance of nonstructural carbohydrates during the 2015–2016 El Niño drought across a tropical forest precipitation gradient. *Plant. Cell Environ.* **42**, 1705–1714 (2019).
36. Subasinghe Achchige, Y. M., Volkova, L., Drinnan, A. & Weston, C. J. A quantitative test for heat-induced cell necrosis in vascular cambium and secondary phloem of *Eucalyptus obliqua* stems. *J. Plant Ecol.* **14**, 160–169 (2021).
37. Tebaldi, C. et al. Climate model projections from the Scenario Model Intercomparison Project (ScenarioMIP) of CMIP6. *Earth Syst. Dyn.* **12**, 253–293 (2021).
38. Rowland, L. et al. Death from drought in tropical forests is triggered by hydraulics not carbon starvation. *Nature* **528**, 119–122 (2015).
39. Vargas Zeppetello, L. R. et al. Large scale tropical deforestation drives extreme warming. *Environ. Res. Lett.* **15**, 84012 (2020).
40. Araújo, I. et al. Trees at the Amazonia–Cerrado transition are approaching high temperature thresholds. *Environ. Res. Lett.* **16**, 34047 (2021).

Publisher's note Springer Nature remains neutral with regard to jurisdictional claims in published maps and institutional affiliations.

Springer Nature or its licensor (e.g. a society or other partner) holds exclusive rights to this article under a publishing agreement with the author(s) or other rightsholder(s); author self-archiving of the accepted manuscript version of this article is solely governed by the terms of such publishing agreement and applicable law.

© The Author(s), under exclusive licence to Springer Nature Limited 2023

Methods

Field data

We estimated canopy temperature at the KM 83 eddy covariance tower in the Tapajos region of Brazil^{41–43} using a pyrgeometer (Kipp and Zonen) mounted at 64 m to measure the upwelling longwave radiation ($L \uparrow$ in $W m^{-2}$) with an estimated radiative-flux footprint of 8,000 m^2 (ref. 21). Data were collected every 2 s and averaged over 30-min intervals between August 2001 and March 2004. We estimated canopy temperature with the following equation:

$$\text{Canopy temperature (}^{\circ}\text{C)} = (L \uparrow / (E \times 5.67e^{-8}))^{0.25} - 273.15 \quad (1)$$

We chose an emissivity value (E) of 0.98 for the tower data, as this was the most common value used in the ECOSTRESS data (SDS_Emis1-5 (ECO2LSTE.001) and the broader literature for tropical forests⁴⁴. We compared canopy temperature derived from the pyrgeometer to eddy covariance-derived latent heat fluxes (flux footprint of approximately 1 km^2), air temperature at 40 m, which is the approximate canopy height (model O76B, Met One; and model 107, Campbell Scientific) and soil moisture at depths of 40 cm (model CS615, Campbell Scientific). Further details on instrumentation and eddy covariance processing can be found in refs. 41,43. This site was selectively logged, which had a minor overall effect on the forest⁴⁵, but did not affect any trees near the tower.

Leaf thermocouple data. We measured canopy leaf temperature at a 30-m canopy walk-up tower between July to December of 2004 and July to December of 2005 at the same site. We initially placed 50 thermocouples on canopy-exposed leaves of *Sextonia rubra*, *Micropholis* sp., *Lecythis lurida* (originally published in Doughty and Goulden⁸). Fine-wire thermocouples (copper constantan 0.005 Omega) were attached to the underside of leaves by threading the wire through the leaf and inserting the end of the thermocouple into the abaxial surface. The thermocouples were wired into a multiplexer attached to a data logger (models AM25T and 23X, Campbell Scientific) and the data were recorded at 1 Hz. Additional upper canopy leaf thermocouple data from Brazil¹⁷, Puerto Rico¹⁸, Panama¹⁹, Atlantic forest Brazil¹⁶ and Australia²⁰ were generally collected in a similar manner.

Satellite data

ECOSTRESS data (ECO2LSTE.001). The ECOSTRESS mission is a thermal infrared multispectral scanner with five spectral bands at 8.28, 8.63, 9.07, 10.6 and 12.05 μm . The sensor has a native spatial resolution of 38 × 68 m, resampled to 70 × 70 m, and a swath width of 402 km (53°). Data were collected from an average altitude of 400 ± 25 km on the International Space Station. ECOSTRESS is an improvement over other thermal sensors because no other sensors provide thermal infrared data with sufficient spatial, temporal and spectral resolution to reliably estimate LST at the local-to-global scale for a diurnal cycle⁴⁶. To ensure the highest quality data, we used ECOSTRESS quality flag 3520, which identifies the best-quality pixels (no cloud detected), a minimum–maximum difference (MMD) indicative of vegetation or water⁴⁷, and nominal atmospheric opacity. We accessed ECOSTRESS LST data through AppEEARS (<https://lpdaac.usgs.gov/tools/appeears/>) for the following products and periods: SDS_LST (ECO2LSTE.001) from a long longitudinal swath of the Amazon for 25 December 2018 to 20 July 2020 (Supplementary Fig. 1a, red box) and then a larger area of the western Amazon for 18 September to 29 September 2019 (Supplementary Fig. 1a, green box), Central Africa for 1 August to 30 August 2019 (Supplementary Fig. 1b) and Southeast Asia for 15 January to 30 February 2020 (Supplementary Fig. 1c). The dates were chosen as all ECOSTRESS data available at the start of the study for the smaller regions and for warm periods with low soil moisture for the larger areas. We calculated ‘peak median’, which is defined as the average of the highest three medians of each granule (that is, for

the Amazon in Supplementary Fig. 1a, there were 934 granules) for each hour period.

Comparison of LST data. We compared ECOSTRESS LST to VIIRS LST (VNP21A1D.001) and MODIS LST (MYD11A1.006). A more detailed comparison and description of these sensors can be found in Hulley et al.¹⁵. Details for the sensors and quality flags used are given in Supplementary Table 1. Broadly, G1 for ECOSTRESS and VIIRS is classified as vegetation (using emissivity) and of medium quality. G2 is classified as vegetation, but of the highest quality. MODIS landcover classifies this region as almost entirely broadleaf evergreen vegetation, but using MMD (emissivity), only 18% (VIIRS) and 12% (ECOSTRESS) of the data are classified as vegetation, rather than as soils and rocks (Supplementary Table 2). Therefore, we used the vegetation classification (from MMD) as a very conservative estimate of complete forest canopy cover and not farms, urban or degraded forest where rocks or soils are more likely to appear to satellites.

SMAP data. To estimate pantropical soil moisture, we used the SMAP sensor and the product Geophysical_Data_sm_rootzone (SPL4SMGP.005). SMAP measurements provide remote sensing of soil moisture in the top 5 cm of the soil⁴⁸ and the L4 products combine SMAP observations and complementary information from various sources. We accessed SMAP data from AppEEARS for the following products and periods: the Amazon for 25 December 2018 to 20 July 2020 (Supplementary Fig. 1a), Central Africa for 25 December 2019 to 20 July 2020 (Supplementary Fig. 1b) and Borneo for 25 December 2018 to 20 July 2020 (Supplementary Fig. 1c).

Warming experiments

For model validation, we used the results of three upper canopy leaf and branch warming experiments of 2 °C (Brazil)¹⁷, 3 °C (Puerto Rico)¹⁸ and 4 °C (Australia)²⁰. The first experiment (Brazil) were four individual leaf-resistant heaters on each of six different upper canopy species at the Floresta Nacional (FLONA) do Tapajos as part of the Large-Scale Biosphere–Atmosphere Ecology Program in Santarem, Brazil¹⁷. On the same six species, black plastic passively heated branches by an average of approximately 2 °C. Initially, heat balance sap flow sensors and the passive heaters were added to 40 branches, but we had confidence in the data from 9 heated and 4 control in the final analysis. The second experiment (Puerto Rico) had two species (*Ocotea sintenisii* (Mez) Alain and *Guarea guidonia* (L.) Sleumer where leaves were heated by 3 °C at the Tropical Responses to Altered Climate Experiment canopy tower site at the Sabana Field Research Station, Luquillo, Puerto Rico¹⁸. The final experiment (Australia), which increased leaf temperatures by 4 °C, was conducted at Daintree Rainforest Observatory in Cape Tribulation, Far North Queensland, Australia²⁰. Leaf heaters were installed using a pair of 30-G copper-constantan thermocouples, one reference leaf and one heated with a target temperature differential of 4 °C. There were two pairs in the upper canopy of each tree crown installed in 2–3 individuals across four species with the thermocouples installed on the underside of the leaves. Two absolute 36-G copper-constantan thermocouples were installed in each species to measure the leaf temperatures of the reference leaves. Thermocouple wires connected into an AM25T multiplexer from Campbell Scientific connected to a CR1000 Campbell datalogger. More details about the experiment and sensors can be found in ref. 20.

Model

We created a model of individual leaves on a tree (100 × 100 grid where each pixel is a leaf) using MATLAB (Mathworks version 2022a) to estimate the upper limit of tropical canopy temperatures with projected changes in climate. At the start of the simulation, we randomly applied the measured distribution (ambient, Fig. 1c) of canopy leaf temperatures of more than 31.2 °C (chosen to give a mean canopy temperature

of 33.1 ± 0.4 °C, matching the canopy average; Fig. 1b) to the entire grid. Each year, we increased the mean air temperatures by 0.03 °C to simulate a warming planet. As air temperatures reached +2, 3 and 4 °C, we applied the leaf temperature distributions (but subtracted out the air temperature increases) from the different warming experiments (+2 °C (Brazil), +3 °C (Puerto Rico) and +4 °C (Australia), respectively (Extended Data Fig. 4)). We ran the model at a daily time step with leaves flushing once a year (all dead leaves reset to living each year).

In addition, to take into account the effect of climate inter-annual variation—specifically drought—these mean canopy temperatures were further increased or decreased by deviations from mean maximum air temperatures at 40 m pulled each day from the Tapajos eddy covariance tower^{41–43} and soil moisture at a depth of 40 cm ($\text{m}^3 \text{m}^{-3}$), which controlled canopy temperatures following equation (2) (Extended Data Fig. 2a).

$$\text{Canopy temperature (}^\circ\text{C)} = 46.5 - 33.6 \times \text{soil moisture}(\text{m}^3 \text{m}^{-3}) \quad (2)$$

For example, in a non-drought year, on a day where max air temperatures were 0.1 °C higher than average and soil moisture was $0.01 \text{ m}^3 \text{m}^{-3}$ lower than average (which would add 0.3 °C to canopy temperatures (equation (2))), we would add 0.4 °C to the grid canopy temperature that day. Every year, there was a 10% random probability of either a minor (80% probability) drought, which reduced soil moisture by $0.1 \text{ m}^3 \text{m}^{-3}$ and increased air temperatures by 0.5 °C or severe drought (20% probability), which reduced soil moisture by $0.2 \text{ m}^3 \text{m}^{-3}$ and increased air temperatures by 1 °C. This is similar to the Amazon-wide temperature increases during the last El Niño⁶.

If an individual leaf temperature increases to above 46.7 °C (T_{crit}), the leaf died, following Slot et al.¹. Previous research has suggested that irreversible damage could begin at 45 °C³⁰ and T_{50} for tropical species is 49.9 °C¹, and we used these values in a sensitivity study. We further explored the effect of duration of T_{crit} on mortality in a sensitivity study (ranging between needing a single exposure to four exposures to T_{crit} to die). Over the season, if a leaf died, then it did not contribute towards canopy evapotranspiration. We ran simulations as a 3D canopy with an LAI of 5; if the top leaf died, then it was replaced by a shade-adapted leaf with a T_{crit} of 1 °C lower⁴⁹. If each of the 5 LAIs died, then all leaves in that grid cell were dead and canopy evaporative cooling decreased by that percentage. Several lines of evidence suggest that under normal hydraulic conditions, when radiation load increases from approximately 350 to 1,100 W m^{-2} (for example, between shady and sunny conditions), average canopy temperature increases by approximately 3 °C and therefore evaporative cooling for a full 1,100 W m^{-2} is approximately 4.4 °C^{8,21} (we vary this in a sensitivity study between 3.7 and 5.1 °C). For example, if, over a year, 1,000 leaves (10% of all leaves) surpass T_{crit} and die, evaporative cooling for all leaves in the grid will be reduced by 10% ($1,000/(100 \times 100 \text{ grid})$) or 0.44 °C and 0.44 °C will be added to mean canopy temperature. Therefore, mean canopy temperature could heat up by a maximum of 4.4 °C either due to a reduction of soil moisture or from an increase in dead leaves. We ran each simulation until the point where all leaves were dead, and repeated this 30 times. We assumed loss of tree function following the death of all leaves, but we discuss this further in the 'Discussion' section. We then ran sensitivity studies for several of the key variables (bold indicates the standard model

parameter) including: drought (0.05, **0.1**, to $0.2 \text{ m}^3 \text{m}^{-3}$ decrease in soil moisture), change in T_{crit} (45, **46.7**, 49.9 °C), T_{crit} range ($100 \times 100 \text{ grid} = \text{random distribution of } 46.7 \pm 2$, **$100 \times 100 \text{ grid} = 46.7 \pm 0$**), maximum evaporative cooling (3.7, **4.4** °C), (T_{crit} duration (**exceed T_{crit} once**, exceed T_{crit} more than three times) and soil moisture coefficient (**-33.6** -38.2; that is, change the slope from Extended Data Fig. 2a by $\pm 1 \text{ s.d.}$).

Reporting summary

Further information on research design is available in the Nature Portfolio Reporting Summary linked to this article.

Data availability

We provide key data in the supplementary information. Data and code to produce all figures are available at <https://doi.org/10.5061/dryad.fqz612jx1>. Source data are provided with this paper.

Code availability

Data and code to produce all figures are available at <https://doi.org/10.5061/dryad.fqz612jx1>.

1. Miller, S. D. et al. Biometric and micrometeorological measurements of tropical forest carbon balance. *Ecol. Appl.* **14**, 114–126 (2004).
2. da Rocha, H. R. et al. Seasonality of water and heat fluxes over a tropical forest in eastern Amazonia. *Ecol. Appl.* **14**, 22–32 (2004).
3. Goulden, M. L. et al. Diel and seasonal patterns of tropical forest CO_2 exchange. *Ecol. Appl.* **14**, 42–54 (2004).
4. Jin, M. & Liang, S. An improved land surface emissivity parameter for land surface models using global remote sensing observations. *J. Clim.* **19**, 2867–2881 (2006).
5. Miller, S. D. et al. Reduced impact logging minimally alters tropical rainforest carbon and energy exchange. *Proc. Natl Acad. Sci. USA* **108**, 19431–19435 (2011).
6. Xiao, J., Fisher, J. B., Hashimoto, H., Ichii, K. & Parazoo, N. C. Emerging satellite observations for diurnal cycling of ecosystem processes. *Nat. Plants* **7**, 877–887 (2021).
7. Kealy, P. S. & Hook, S. J. Separating temperature and emissivity in thermal infrared multispectral scanner data: implications for recovering land surface temperatures. *IEEE Trans. Geosci. Remote Sens.* **31**, 1155–1164 (1993).
8. Reichle, R., De Lannoy, G., Koster, R. D., Crow, W. T. & Kimball, J. S. SMAP L4 9 km EASE-grid surface and root zone soil moisture geophysical data, version 3. National Snow and Ice Data Center <https://doi.org/10.5067/B59DT1D5UMB4> (2017).
9. Slot, M., Krause, G. H., Krause, B., Hernández, G. G. & Winter, K. Photosynthetic heat tolerance of shade and sun leaves of three tropical tree species. *Photosynth. Res.* **141**, 119–130 (2019).

Acknowledgements Support was provided by the ECOSTRESS mission and NASA Research Opportunities in Space and Earth Science grant numbers 80NSSC20K0216, 80NSSC19K0206 and 80NSSC21K0191. S.F. and E.G. acknowledge Natural Environmental Research Council grant NE/V008366/1. K.C. acknowledges the Australian Research Council grant DE160101484.

Author contributions C.E.D., G.R.G., I.O.M., Y.M. and J.B.F. designed the study. C.E.D. and J.M.K. analysed the remote sensing data. C.E.D., M.L.G., H.R.d.R., S.D.M., S.F., E.G., C.R.-S., M.S., K.R.C., K.Y.C., K.B.M. and A.W.C. collected and analysed the empirical data. C.E.D. created the model. C.E.D. and B.C.W. prepared the public data and code. C.E.D. wrote the paper with contributions from G.R.G., K.Y.C., J.B.F. and I.O.M.

Competing interests The authors declare no competing interests.

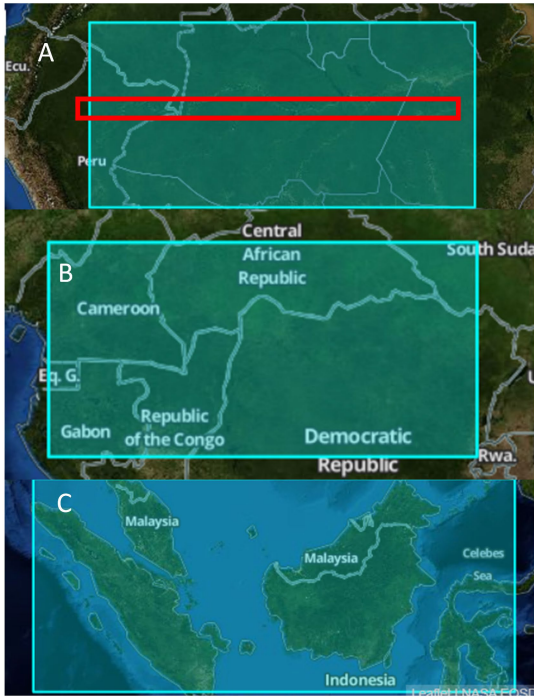
Additional information

Supplementary information The online version contains supplementary material available at <https://doi.org/10.1038/s41586-023-06391-z>.

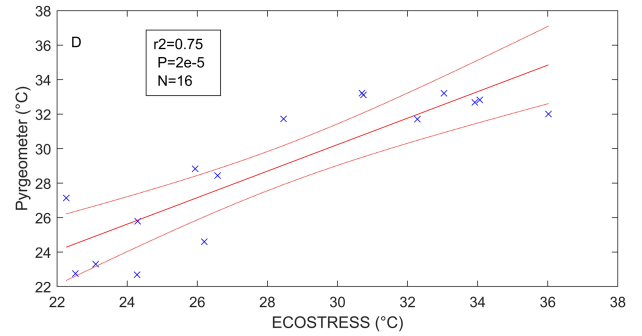
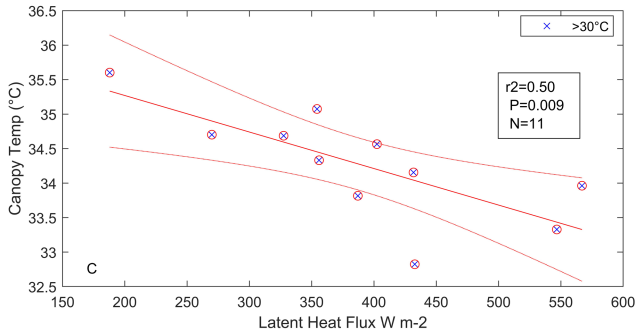
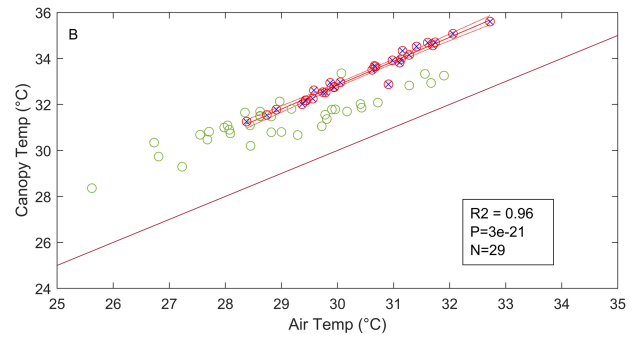
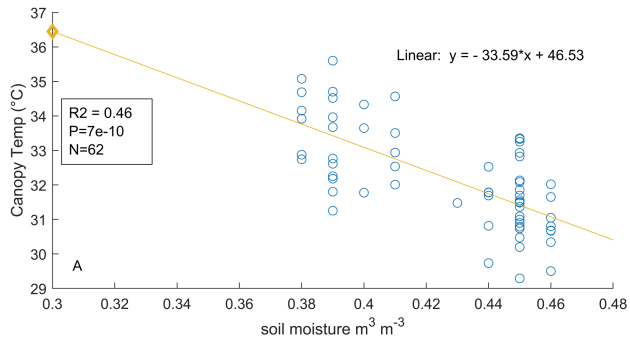
Correspondence and requests for materials should be addressed to Christopher E. Doughty.

Peer review information Nature thanks Ben Bond-Lamberty, David Schimel and the other, anonymous, reviewer(s) for their contribution to the peer review of this work. Peer reviewer reports are available.

Reprints and permissions information is available at <http://www.nature.com/reprints>.



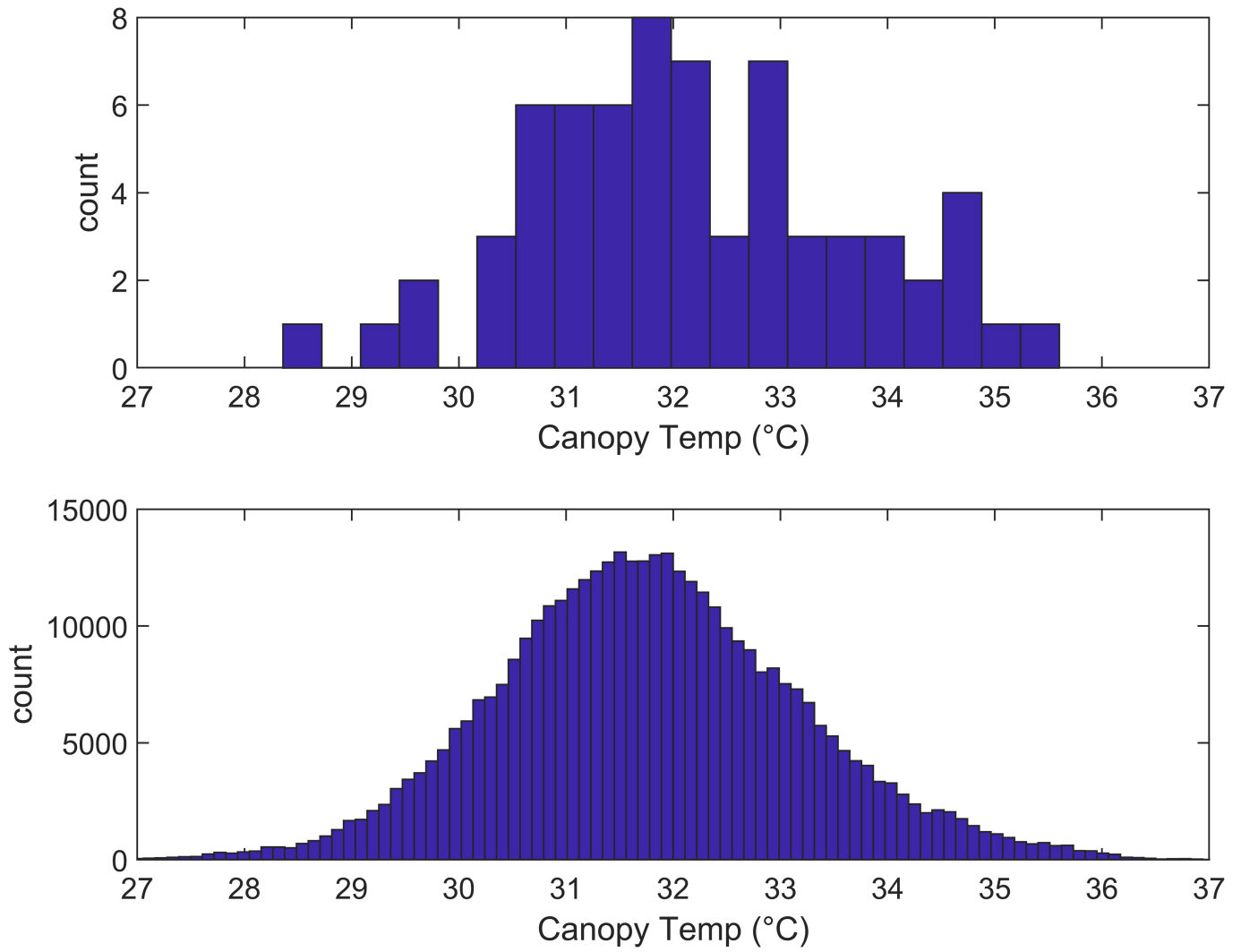
Extended Data Fig. 1 | Regions of interest. Tropical forest regions in A) Amazon, B) Central Africa and C) SE Asia used for the retrieval of ECOSTRESS LST and SMAP data. The red area was used to ground-truth ECOSTRESS LST with the pyrogeometer.



Extended Data Fig. 2 | Impacts on canopy temperature. (A) Linear regression of canopy temperature versus soil moisture (40 cm depth) at the km 83 eddy covariance tower ($r^2 = 0.46$, $P = 7e-10$, $N = 62$). (B) Linear regression of canopy temperature as a function of air temperature during sunny periods during the wet (green circles) and dry (red circles) season at the km 83 eddy covariance tower in the Tapajos region of Brazil. Red line shows a linear fit for the dry

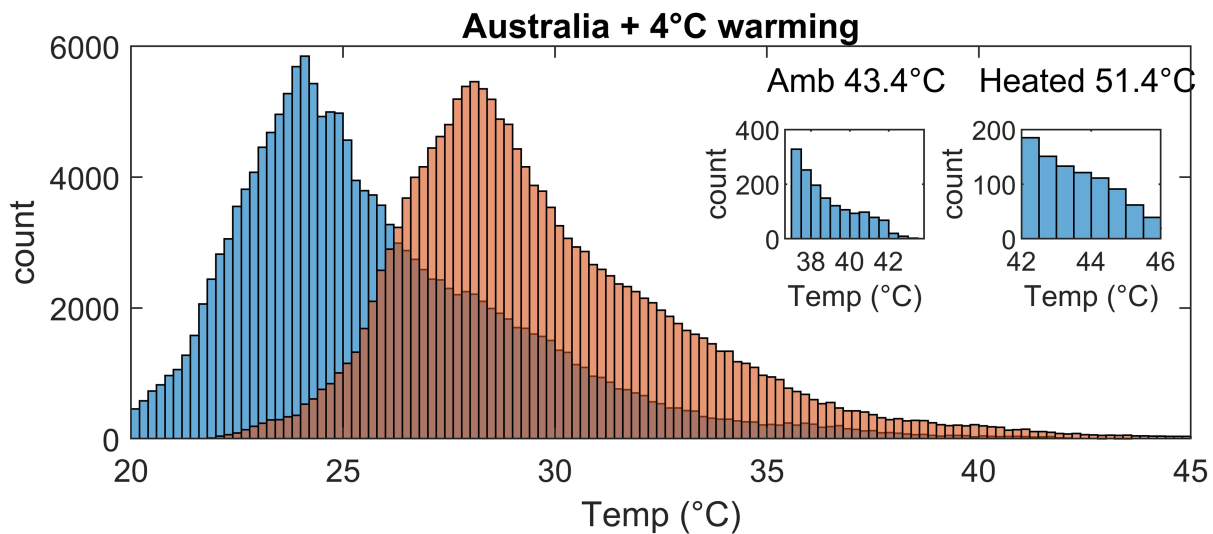
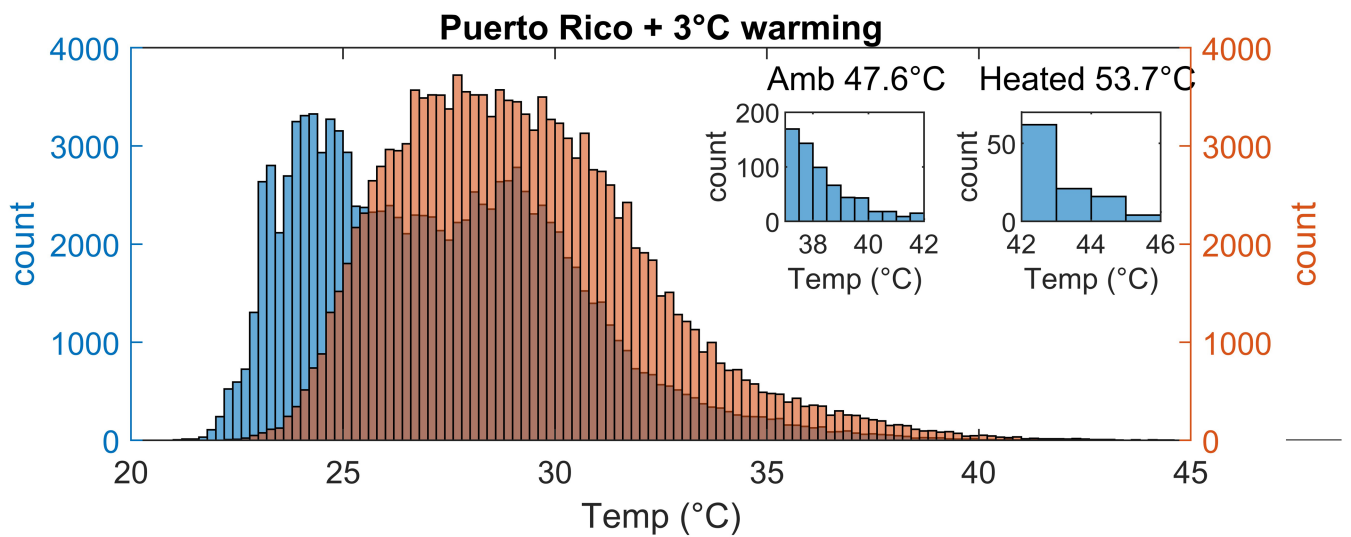
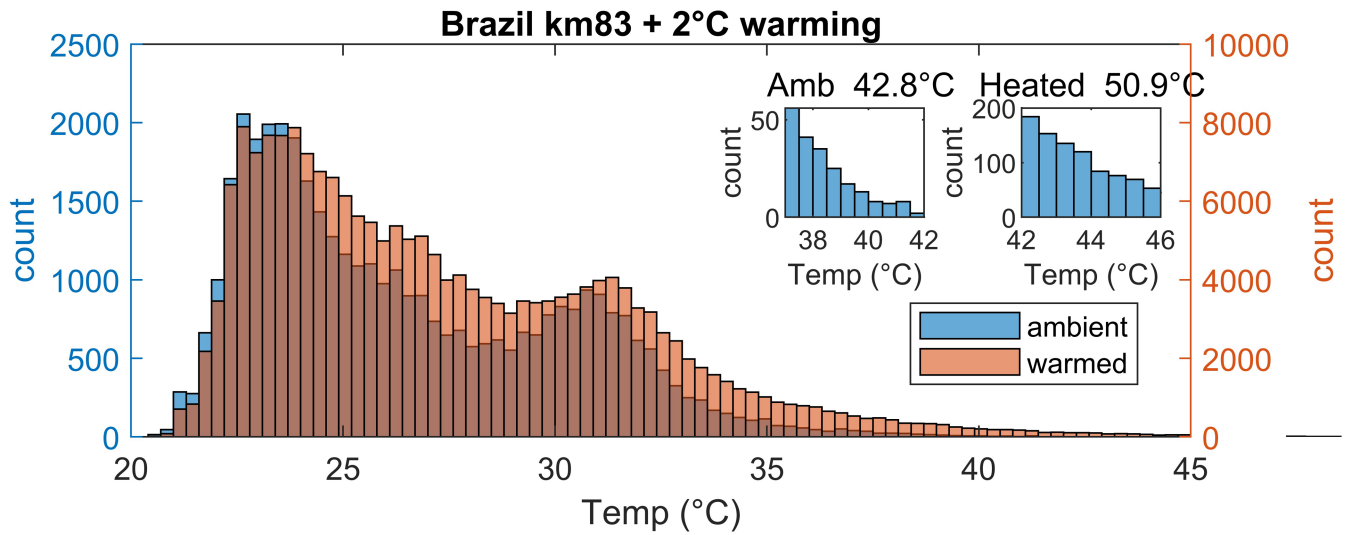
season ($r^2 = 0.96$, $P = 3e-21$, $N = 29$) and the lower line is a one-to-one line. (C) Linear regressions of canopy temperature as a function of latent heat flux for warm ($>30^\circ\text{C}$) periods ($r^2 = 0.50$, $P = 0.009$, $N = 11$) at the km 83 eddy covariance tower in the Tapajos region of Brazil. (D) Linear regression ($r^2 = 0.75$, $P = 2e-5$, $N = 16$) using data from Fig. 1a comparing ECOSTRESS dry season to pyrgometer dry season data from the Tapajos (Km 83).

Article



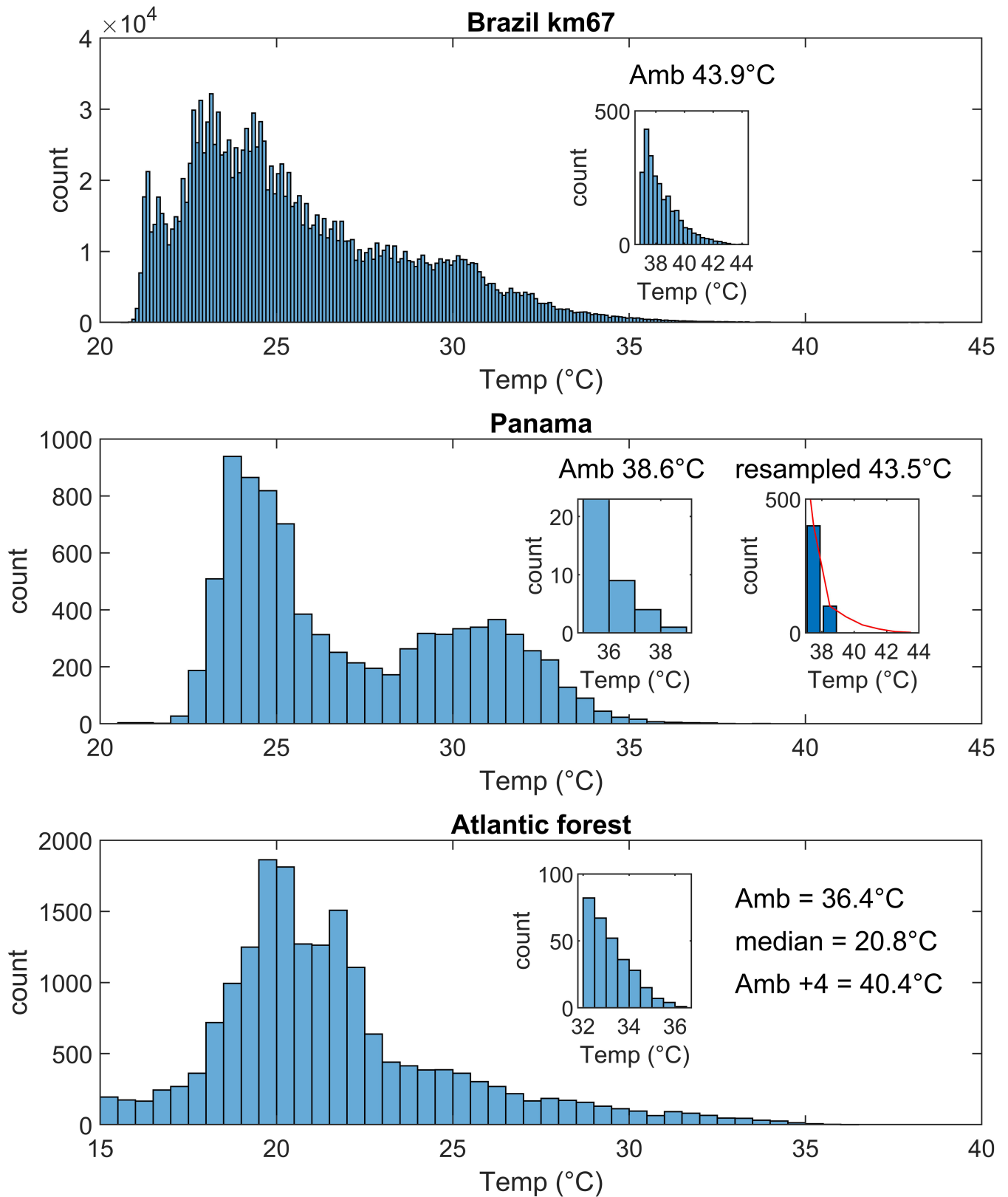
Extended Data Fig. 3 | Histograms of canopy temperature. Histograms of the canopy temperatures as (top) 30 min average periods and (bottom) two second instantaneous observations, where total shortwave energy load is

$>1000 \text{ W m}^{-2}$, as measured by a downward facing pyrgometer in the Tapajos region of Brazil.



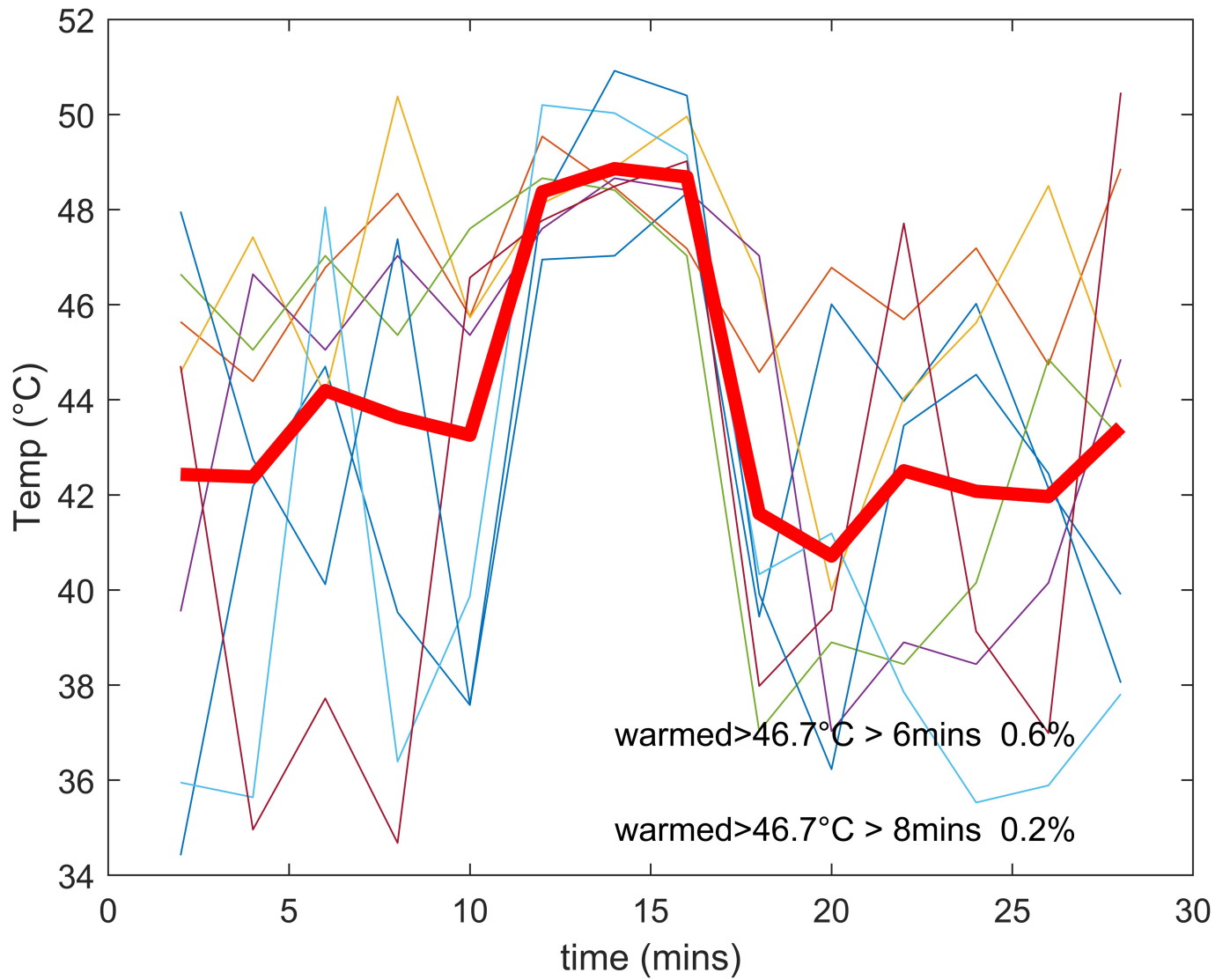
Extended Data Fig. 4 | Leaf thermocouple data from warming experiments. Canopy top tropical leaf thermocouple measurements for normal (blue) and warmed leaves (red) for Brazil (+2°C), Puerto Rico (+3°C), and Australia (+4°C).

Insets show the long tail distribution of temperatures and text records the highest leaf temperature.

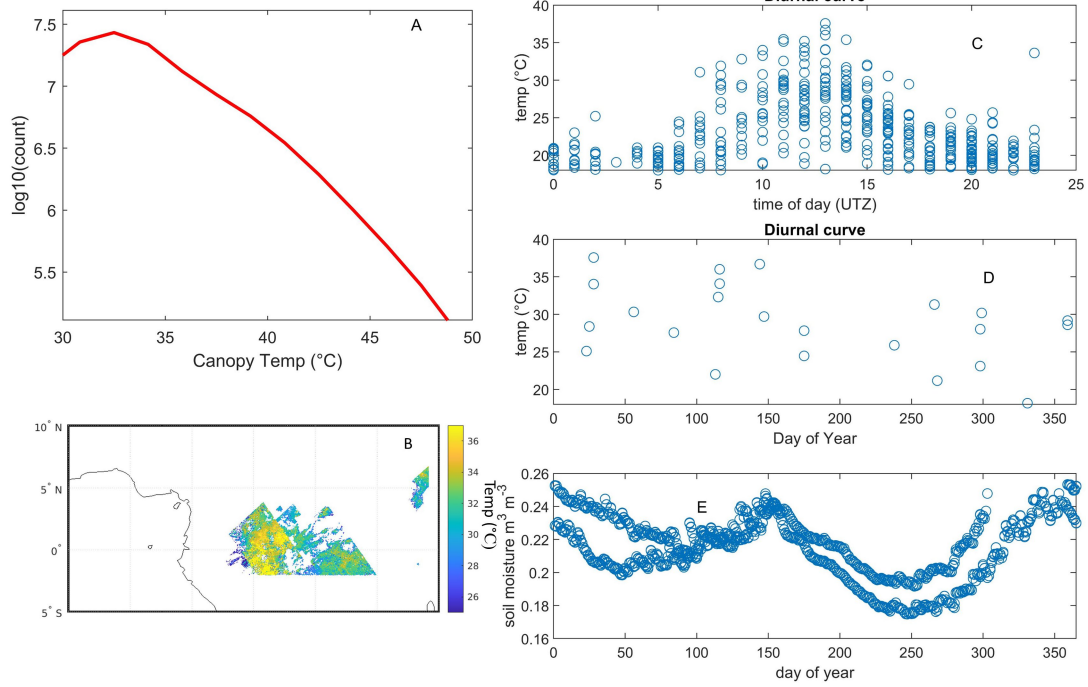


Extended Data Fig. 5 | Leaf thermocouple data. Canopy top tropical leaf thermocouple measurements for (top) Brazil km 67, (middle) Panama and (bottom) the Atlantic Forest in Brazil. Insets show the long tail distribution of temperatures and text records the highest leaf temperature. The resampled

assumes a similar number of samples ($-N = 400$) at 38 °C for both sites and fits a curve to extrapolate the long tail. The Atlantic forest is a cooler forest (at -1000 m) and the median temperature of the Amazon is -4 °C higher than the Atlantic forest.

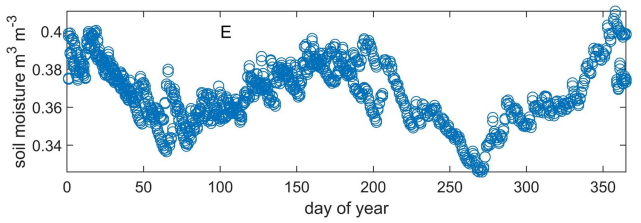
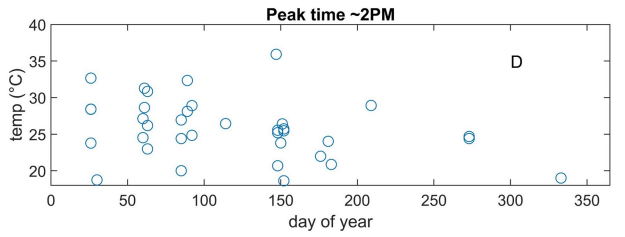
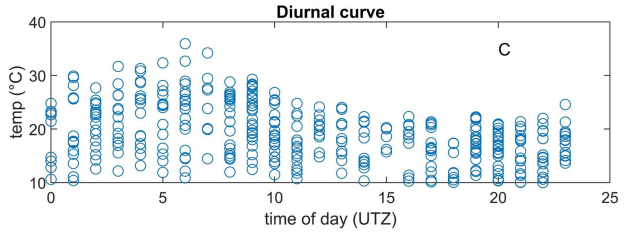
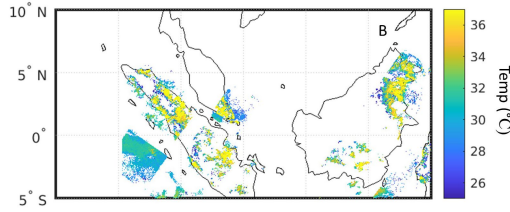
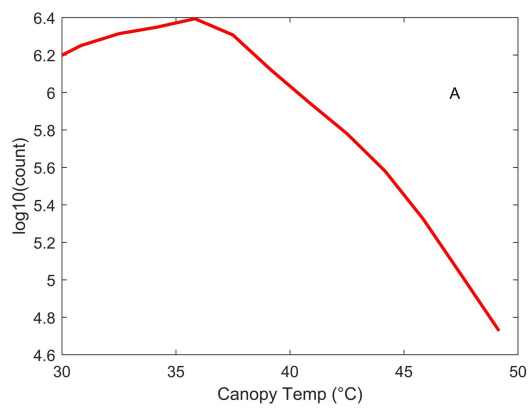


Extended Data Fig. 6 | Duration of warming. Periods when the leaves were warmed by >8 min during the Tapajos warming experiment for individual leaves (thin lines) and averaged (thick red line). Text in figure indicates the percent of time leaves exceeded T_{crit} for greater than 6 and 8 min.



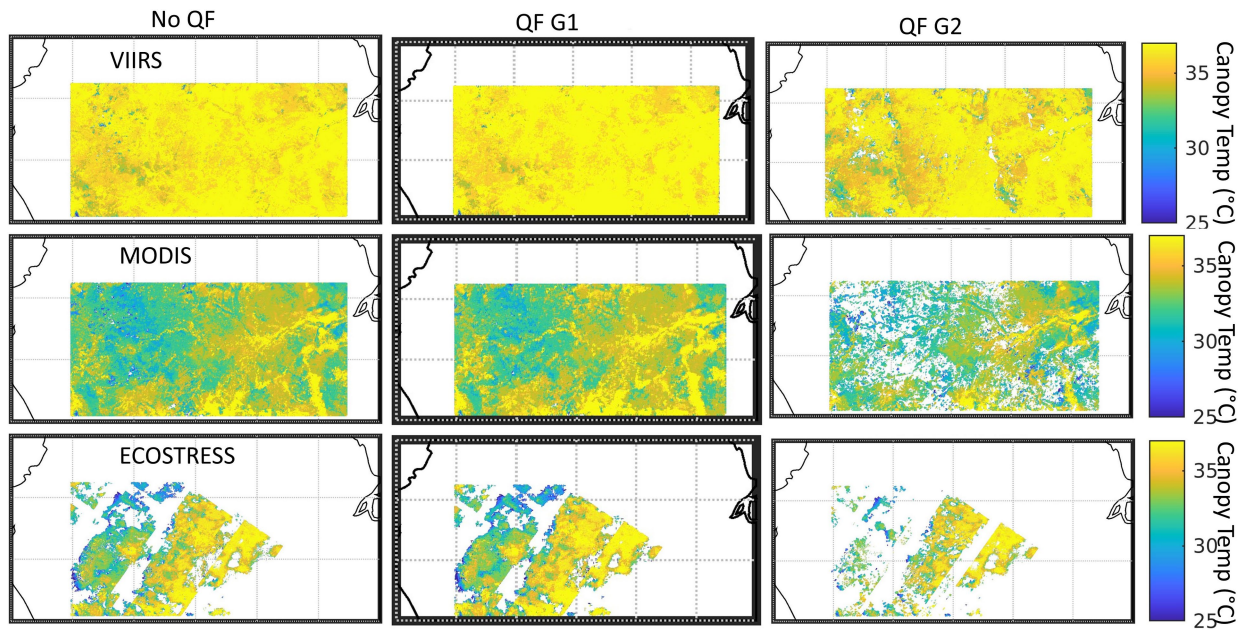
Extended Data Fig. 7 | Finding African peak temperatures. Procedure for finding peak canopy temperatures using ECOSTRESS data for central Africa. (A) Log10 histogram of temperatures for (B) a region of Central Africa.

A diurnal curve showing all ECOSTRESS LST data for central Africa versus (C) time of day and (D) time of year. (E) SMAP soil moisture (m³ m⁻³) data showing periods of dry weather.



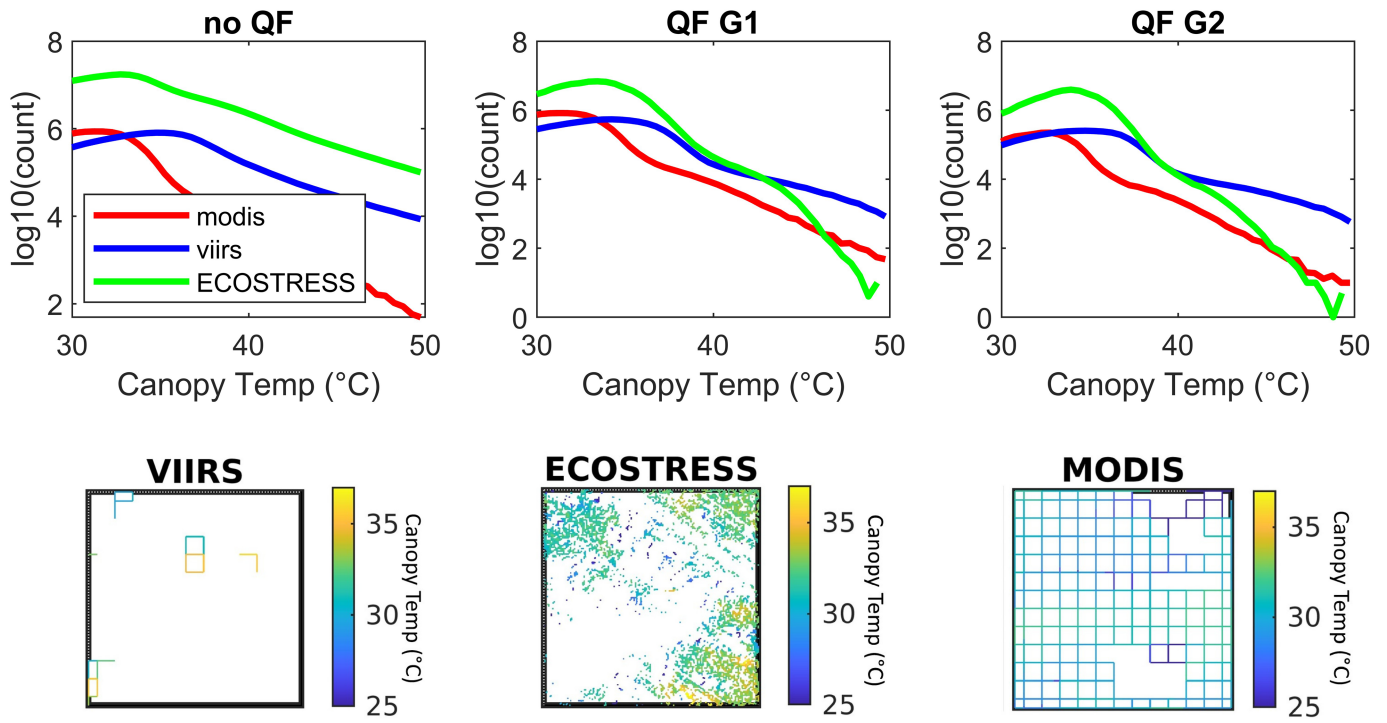
Extended Data Fig. 8 | Finding SE Asian peak temperatures. Procedure for finding peak canopy temperatures using ECOSTRESS data for SE Asia. (A) Log10 histogram of temperatures for (B) a region of Central Africa.

A diurnal curve showing all ECOSTRESS LST data for SE Asia versus (C) time of day and (D) time of year. (E) SMAP soil moisture data ($\text{m}^3 \text{m}^{-3}$) showing periods of dry weather.



Extended Data Fig. 9 | Comparison of LST temperature data. We show the spatial distribution of LST data for three sensors (VIIRS, MODIS, and ECOSTRESS) for similar time periods (Sept 18–28, 2019) for similar areas in the Amazon basin. The difference between the left, middle and right are different data quality flags for no flag (left), QF g1 from Supplementary Table 1 (middle) and QF g2 (right). We used three levels of quality flags (ECOSTRESS – G1 - 3522

and 3520, G2=3520, VIIRS – G1 – 12001, 15841, 11745, 32225 and G2 = 32225, and MODIS – G1 - 0 and 65 and G2 - 0) for the region depicted in Extended Data Fig. 1a during the same period (18 September to 28 September 2019). Quality flags were complex with 136 for ECOSTRESS and 229 for VIIRS (but only 8 for MODIS).



Extended Data Fig. 10 | Histogram of LST temperature data. (top) We show log₁₀ histograms of LST data for three sensors (VIIRS, MODIS, and ECOSTRESS) for similar time periods (Sept 18–28, 2019) for similar areas in the Amazon basin. The difference between the left, middle and right are different data quality flags for no flag (left), QF g1 from Supplementary Table 1 (middle) and QF g2 (right). We used three levels of quality flags (ECOSTRESS – G1 - 3522 and 3520, G2=3520, VIIRS – G1 – 12001, 15841, 11745, 32225 and G2= 32225, and MODIS – G1 - 0 and 65 and G2 - 0) for the region depicted in Extended Data Fig. 1a during the same period (18 September to 28 September 2019). (bottom) - A scaled in comparison for the same dataset showing the much higher resolution of ECOSTRESS versus VIIRS and MODIS LST.

Reporting Summary

Nature Portfolio wishes to improve the reproducibility of the work that we publish. This form provides structure for consistency and transparency in reporting. For further information on Nature Portfolio policies, see our [Editorial Policies](#) and the [Editorial Policy Checklist](#).

Statistics

For all statistical analyses, confirm that the following items are present in the figure legend, table legend, main text, or Methods section.

- | n/a | Confirmed |
|-------------------------------------|--|
| <input type="checkbox"/> | <input checked="" type="checkbox"/> The exact sample size (n) for each experimental group/condition, given as a discrete number and unit of measurement |
| <input checked="" type="checkbox"/> | <input type="checkbox"/> A statement on whether measurements were taken from distinct samples or whether the same sample was measured repeatedly |
| <input type="checkbox"/> | <input checked="" type="checkbox"/> The statistical test(s) used AND whether they are one- or two-sided
<i>Only common tests should be described solely by name; describe more complex techniques in the Methods section.</i> |
| <input type="checkbox"/> | <input checked="" type="checkbox"/> A description of all covariates tested |
| <input checked="" type="checkbox"/> | <input type="checkbox"/> A description of any assumptions or corrections, such as tests of normality and adjustment for multiple comparisons |
| <input type="checkbox"/> | <input checked="" type="checkbox"/> A full description of the statistical parameters including central tendency (e.g. means) or other basic estimates (e.g. regression coefficient) AND variation (e.g. standard deviation) or associated estimates of uncertainty (e.g. confidence intervals) |
| <input type="checkbox"/> | <input checked="" type="checkbox"/> For null hypothesis testing, the test statistic (e.g. F , t , r) with confidence intervals, effect sizes, degrees of freedom and P value noted
<i>Give P values as exact values whenever suitable.</i> |
| <input checked="" type="checkbox"/> | <input type="checkbox"/> For Bayesian analysis, information on the choice of priors and Markov chain Monte Carlo settings |
| <input checked="" type="checkbox"/> | <input type="checkbox"/> For hierarchical and complex designs, identification of the appropriate level for tests and full reporting of outcomes |
| <input checked="" type="checkbox"/> | <input type="checkbox"/> Estimates of effect sizes (e.g. Cohen's d , Pearson's r), indicating how they were calculated |

Our web collection on [statistics for biologists](#) contains articles on many of the points above.

Software and code

Policy information about [availability of computer code](#)

- | | |
|-----------------|---|
| Data collection | We created custom code using matlab to analyze our data and this code and the corresponding data is available through a link listed in the paper. |
| Data analysis | We created custom code using matlab to analyze our data and this code and the corresponding data is available through a link listed in the paper. |

For manuscripts utilizing custom algorithms or software that are central to the research but not yet described in published literature, software must be made available to editors and reviewers. We strongly encourage code deposition in a community repository (e.g. GitHub). See the Nature Portfolio [guidelines for submitting code & software](#) for further information.

Data

Policy information about [availability of data](#)

All manuscripts must include a [data availability statement](#). This statement should provide the following information, where applicable:

- Accession codes, unique identifiers, or web links for publicly available datasets
- A description of any restrictions on data availability
- For clinical datasets or third party data, please ensure that the statement adheres to our [policy](#)

We provide key data as a .csv file as a supplement and all other data and code through a link listed in the paper.

Human research participants

Policy information about [studies involving human research participants and Sex and Gender in Research](#).

Reporting on sex and gender

Use the terms *sex* (biological attribute) and *gender* (shaped by social and cultural circumstances) carefully in order to avoid confusing both terms. Indicate if findings apply to only one sex or gender; describe whether sex and gender were considered in study design whether sex and/or gender was determined based on self-reporting or assigned and methods used. Provide in the source data disaggregated sex and gender data where this information has been collected, and consent has been obtained for sharing of individual-level data; provide overall numbers in this Reporting Summary. Please state if this information has not been collected. Report sex- and gender-based analyses where performed, justify reasons for lack of sex- and gender-based analysis.

Population characteristics

Describe the covariate-relevant population characteristics of the human research participants (e.g. age, genotypic information, past and current diagnosis and treatment categories). If you filled out the behavioural & social sciences study design questions and have nothing to add here, write "See above."

Recruitment

Describe how participants were recruited. Outline any potential self-selection bias or other biases that may be present and how these are likely to impact results.

Ethics oversight

Identify the organization(s) that approved the study protocol.

Note that full information on the approval of the study protocol must also be provided in the manuscript.

Field-specific reporting

Please select the one below that is the best fit for your research. If you are not sure, read the appropriate sections before making your selection.

Life sciences Behavioural & social sciences Ecological, evolutionary & environmental sciences

For a reference copy of the document with all sections, see [nature.com/documents/nr-reporting-summary-flat.pdf](https://www.nature.com/documents/nr-reporting-summary-flat.pdf)

Ecological, evolutionary & environmental sciences study design

All studies must disclose on these points even when the disclosure is negative.

Study description

Here we use data from the new ECOSTRESS sensor to estimate peak pantropical forest canopy temperatures. We begin by ground truthing the satellite data with tower-based pyrgeometer data. We then use these data to determine what causes variation in peak temperatures at the canopy scale and show similar trends driving peak temperatures across all of the Tropics. Critically, we show that for a given canopy temperature, individual leaf temperatures display a "long tail" of values in the distribution, where the temperatures of a few individual leaves far exceed that of the overall canopy, and that this skewed distribution persists under leaf warming experiments of 2, 3 and 4 °C. Finally, we develop a simple empirical model to explore the implications of observed leaf temperatures on the fate of tropical forests under future climate change.

Research sample

We measured canopy leaf temperature at a 30 m canopy walk-up tower in Brazil. Additional upper-canopy leaf thermocouple data from Brazil, Puerto Rico, Panama, Atlantic forest Brazil and Australia, were generally collected in a similar manner. We also used remote sensing data and create an empirical model.

Sampling strategy

The ECOSystem Spaceborne Thermal Radiometer Experiment on Space Station (ECOSTRESS) mission is a thermal infrared (TIR) multispectral scanner with five spectral bands at 8.28, 8.63, 9.07, 10.6, and 12.05 μm . The sensor has a native spatial resolution of 38 m x 68 m, resampled to 70 m x 70 m, and a swath width of 402 km (53°). Data are collected from an average altitude of 400 ± 25 km on the International Space Station (ISS). To ensure the highest quality data, we used ECOSTRESS quality flag 3520, which identifies the best quality pixels (no cloud detected), a minimum-maximum difference (MMD) indicative of vegetation or water (Kealy and Hook 1993), and nominal atmospheric opacity. We accessed ECOSTRESS LST data through the AppEEARS website (<https://lpdaac.usgs.gov/tools/appeears/>) for the following products and periods: SDS_LST (ECO2LSTE.001) from a long longitudinal swath of the Amazon for 25 December 2018 to 20 July 2020 (SI Fig 1a red box) and then a larger area of the western Amazon for 18 September to 29 September 2019 (SI Fig 1a green box), Central Africa for 1 August to 30 August 2019 (SI Fig 1b), and SE Asia for 15 January to 30 February 2020 (SI Fig. 1c). The dates were chosen as all ECOSTRESS data available at the start of the study for the smaller regions and for warm periods with low soil moisture for the larger areas.

Data collection

Authors listed in the paper were responsible for the collection of the leaf temperature data.

Timing and spatial scale

We accessed ECOSTRESS LST data through the AppEEARS website (<https://lpdaac.usgs.gov/tools/appeears/>) for the following products and periods: SDS_LST (ECO2LSTE.001) from a long longitudinal swath of the Amazon for 25 December 2018 to 20 July 2020 (SI Fig 1a red box) and then a larger area of the western Amazon for 18 September to 29 September 2019 (SI Fig 1a green box), Central Africa for 1 August to 30 August 2019 (SI Fig 1b), and SE Asia for 15 January to 30 February 2020 (SI Fig. 1c).

Data exclusions

No data were excluded after following our methodology.

Reproducibility

Randomization

Blinding

Did the study involve field work? Yes No

Field work, collection and transport

Field conditions

Location

Access & import/export

Disturbance

Reporting for specific materials, systems and methods

We require information from authors about some types of materials, experimental systems and methods used in many studies. Here, indicate whether each material, system or method listed is relevant to your study. If you are not sure if a list item applies to your research, read the appropriate section before selecting a response.

Materials & experimental systems

n/a	Involvement
<input checked="" type="checkbox"/>	<input type="checkbox"/> Antibodies
<input checked="" type="checkbox"/>	<input type="checkbox"/> Eukaryotic cell lines
<input checked="" type="checkbox"/>	<input type="checkbox"/> Palaeontology and archaeology
<input checked="" type="checkbox"/>	<input type="checkbox"/> Animals and other organisms
<input checked="" type="checkbox"/>	<input type="checkbox"/> Clinical data
<input checked="" type="checkbox"/>	<input type="checkbox"/> Dual use research of concern

Methods

n/a	Involvement
<input checked="" type="checkbox"/>	<input type="checkbox"/> ChIP-seq
<input checked="" type="checkbox"/>	<input type="checkbox"/> Flow cytometry
<input checked="" type="checkbox"/>	<input type="checkbox"/> MRI-based neuroimaging